arXiv:1710.08297v1 [physics.ao-ph] 23 Oct 2017

Coastal flood implications of 1.5 °C, 2.0 °C, and 2.5 °C temperature stabilization targets in the 21st and 22nd century

D.J. Rasmussen, Klaus Bittermann, Maya K. Buchanan, Scott Kulp, Benjamin H. Strauss, Robert E. Kopp, Michael Oppenheimer

Draft: February 2, 2022

Abstract Sea-level rise (SLR) is magnifying the frequency and severity of coastal flooding. The rate and amount of global mean sea-level (GMSL) rise is a function of the trajectory of global mean surface temperature (GMST). Therefore, temperature stabilization targets (e.g., 1.5 °C and 2.0 °C of warming above pre-industrial levels, as from the Paris Agreement) have important implications for coastal flood risk. Here, we assess differences in the return periods of coastal floods at a global network of tide gauges between scenarios that stabilize GMST warming at 1.5 °C, 2.0 °C, and 2.5 °C above pre-industrial levels. We employ probabilistic, localized SLR projections and long-term hourly tide gauge records to construct estimates of the return levels of current and future flood heights for the 21st and 22nd centuries. By 2100, under 1.5 °C, 2.0 °C, and 2.5 °C GMST stabilization, median GMSL is projected to rise 47 cm with a *very likely* range of 28–82 cm (90% probability), 55 cm (*very likely* 30–94 cm), and 58 cm (*very likely* 36–93 cm), respectively. As an independent comparison, a semi-empirical sea level model calibrated to temperature and GMSL over the past two millennia estimates median GMSL will rise within $< 13\%$ of these projections. By 2150, relative to the 2.0 °C scenario, GMST stabilization of 1.5 °C inundates roughly 5 million fewer inhabitants that currently occupy lands, including 40,000 fewer individuals currently residing in Small Island Developing States. Projected changes to the frequency of current 10-, 100-, and 500-year flood levels are quantified using flood amplification factors that incorporate uncertainty in both historical flood return periods and local SLR. Relative to a 2.0 °C scenario, the reduction in the amplification of the frequency of the 100-yr flood arising from a 1.5 °C GMST stabilization is greatest in the eastern United States and in Europe, with flood frequency amplification being reduced by about half.

1 Introduction

Coastal flooding is a hazard that threatens both life and property. The height of a coastal flood is determined by the combined height of the astronomical tide and storm surge (i.e., the storm tide) and the mean sea level at the time of the event. Rising mean sea levels are already magnifying the frequency and severity of coastal

D.J. Rasmussen, Maya K. Buchanan and Michael Oppenheimer
Woodrow Wilson School of Public & International Affairs, Princeton University, Princeton, NJ, USA. E-mail: dj.rasmussen@princeton.edu

Klaus Bittermann
Department of Earth and Ocean Sciences, Tufts University, Medford, MA, USA and Potsdam Institute for Climate Impact Research, Potsdam, Germany

Scott Kulp and Benjamin H. Strauss
Climate Central, Princeton, NJ, USA

Michael Oppenheimer
Department of Geosciences, Princeton University, Princeton, NJ, USA

Robert E. Kopp
Department of Earth & Planetary Sciences and Institute of Earth, Ocean, & Atmospheric Sciences, Rutgers University, New Brunswick, NJ, USA.

floods (Buchanan et al, 2017; Sweet and Park, 2014) and by the end of the century, coastal floods figure to be among the costliest impacts of climate change in some regions (Hsiang et al, 2017; Diaz, 2016). Sea-level rise (SLR) is expected to permanently inundate low-lying geographic areas (Marzeion and Levermann, 2014; Strauss et al, 2015), but these locations will first experience decreases in the return periods of flood events (e.g., Hunter, 2012; Sweet and Park, 2014).

The rate of global mean sea-level (GMSL) rise depends on the trajectory of global mean surface temperature (GMST; Rahmstorf, 2007; Kopp et al, 2016a; Vermeer and Rahmstorf, 2009), with the long-term committed amount of GMSL largely determined by the stabilized level of GMST (Levermann et al, 2013). Thus, the management of GMST has important implications for regulating future GMSL (Schaeffer et al, 2012), and consequently the frequency and severity of coastal floods. However, GMST stabilization does not imply stabilization of all climate variables. Under stabilized GMST, GSML is expected to continue to rise for centuries, due to the long residence time of anthropogenic CO_2, the thermal inertia of the ocean, and the slow response of large ice sheets to forcing (Clark et al, 2016; Levermann et al, 2013; Held et al, 2010). For instance, Schaeffer et al (2012) found that a 2.0 °C GMST stabilization would lead to a GMSL rise (relative to 2000) of 0.8 m by 2100 and $>$ 2.5 m by 2300, but if the GMST increase were held below 1.5 °C, GMSL rise at the end of the 23rd century would be limited to $\sim$1.5 m. These findings suggest that selection of climate policy goals could have critical long-term consequences for the impacts of future SLR and coastal floods (Clark et al, 2016).

The Paris Agreement seeks to stabilize GMST by limiting warming to "well below 2.0 °C above pre-industrial levels" and to further pursue efforts to "limit the temperature increase to 1.5 °C above pre-industrial levels" (UNFCCC, 2015a). However, a recent literature review under the United Nations Framework Convention on Climate Change (UNFCCC) found the notion that "up to 2.0 °C of warming is considered safe, is inadequate" and that "limiting global warming to below 1.5 °C would come with several advantages" (UNFCCC, 2015b). The advantages and disadvantages of each GMST target as they relate to coastal flooding have not been quantified. This is critical as $>$ 625 million people currently live in low-elevation coastal zones, and population growth is expected in these areas (Neumann et al, 2015). Examining the short- and long-term flood hazard implications of 1.5 °C and 2.0 °C GMST stabilization scenarios, as others have recently done for other climate impacts (e.g. Schleussner et al, 2016a,b; Mitchell et al, 2017; Mohammed et al, 2017), may better inform the policy debate regarding the selection of GMST goals.

In this study, we employ probabilistic, localized SLR projections to assess differences in the frequency of extreme coastal floods across 1.5 °C, 2.0 °C, and 2.5 °C GMST stabilization scenarios at a global network of 194 tide gauges. We use long-term hourly tide gauge records and extreme value theory to estimate present and future return periods of flood events. We extend our analysis through the 22nd century to account for continuing SLR in order to inform multi-century planning and infrastructure investments. Lastly, we assess differences in the exposure of current populations to future SLR under 1.5 °C, 2.0 °C, and 2.5 °C GMST stabilizations.

Various approaches have been used to project GMSL under GMST targets. For instance, Jevrejeva et al (2016) estimate future local SLR under a GMST increase of 2 °C using an RCP8.5 GMST trajectory that passes through 2 °C of warming by mid-century, but this approach likely underestimates SLR relative to a scenario that achieves 2 °C GMST stabilization by 2100 as it neglects the time-lagged, integrated response of the ocean and cryosphere to warming (Clark et al, 2016). More generally, studies that condition future flood projections on the Representative Concentration Pathways (RCPs) may be insufficient for assessing the costs and benefits of climate policy scenarios, such as GMST stabilization targets (e.g., *Section 13.7.2.2* of Church et al, 2013; Buchanan et al, 2017; Hunter, 2012; Tebaldi et al, 2012). The RCPs are designed to be representative of a range of emissions scenarios that result in prescribed anthropogenic radiative forcings by 2100 relative to pre-industrial conditions (e.g., 8.5 Wm^{-2} for RCP8.5). They are not representative of a specific emissions trajectory, climate policy (e.g., GMST target), or socioeconomic and technological change (Moss et al, 2010; van Vuuren et al, 2011).

Semi-empirical sea level (SESL) models (Rahmstorf et al, 2012) can estimate future GMSL rise under various GMST scenarios (e.g., Schaeffer et al, 2012; Bittermann et al, in rev). Unlike their process-based counterparts (e.g., Kopp et al, 2014), SESL models do not explicitly model individual physical components of sea-level change. They are calibrated over a historical period using the observed statistical relationship between GMSL and a climate parameter (such as GMST). Assuming these relationships hold in the future, SESL models project the rate of GMSL change conditional upon a GMST pathway (e.g., Rahmstorf, 2007;

Vermeer and Rahmstorf, 2009; Kopp et al, 2016a). However, SESL models do not produce estimates of local SLR, which are necessary for local risk assessment and adaptation planning because local SLR can substantially differ from the global mean (Milne et al, 2009).

2 Methods

We project global and local sea level under 1.5 °C, 2.0 °C, and 2.5 °C GMST stabilization targets using the component-based, probabilistic, local sea level projection framework from Kopp et al (2014, henceforth K14). We compare the resulting GMSL projections to those from the semi-empirical sea level (SESL) model of Kopp et al (2016a). While SESL models cannot produce local projections of SLR, they can serve as a reference point for evaluating the consistency of process-based projections with historical temperature-GMSL relationships. The flow and sources of information used to construct the local SLR and GMSL projections using the K14 method is depicted in Fig. S-1A, while the flow of information used to generate the SESL projections is provided in Fig. S-1B. Local SLR projections from the K14 approach are combined with historical flood distributions to estimate future return periods of historical flood events (Fig. S-1A).

2.1 Component-based model approach: Global and local sea-level rise projections

Global sea-level change does not occur uniformly. Dynamic ocean processes (Levermann et al, 2005), changes to temperature and salinity (i.e., steric processes), changes in the Earth's rotation and gravitational field associated with water-mass redistribution (e.g., land-ice melt; Mitrovica et al, 2011), and glacial isostatic adjustment (GIA; Farrell and Clark, 1976) cause local sea levels to differ from the global mean. We model local sea level using the K14 framework, but make modifications to accommodate the stratification of Atmosphere-Ocean General Circulation Models (AOGCMs) and RCPs into groups that meet GMST stabilization targets (see Section 2.1.1). AOGCM output from the Coupled Model Intercomparison Project (CMIP) Phase 5 archive (Taylor et al, 2012) forced with the RCPs (to 2100) and their extensions (to 2300) are used for the following SLR components: global mean thermal expansion (TE), local ocean dynamics, and glacial ice contributions (GIC; Marzeion et al, 2012). Antarctic Ice Sheet (AIS) and the Greenland Ice Sheet (GIS) contributions are estimated using a combination of the Intergovernmental Panel on Climate Change's (IPCC) Assessment Report 5 (AR5) projections of ice sheet dynamics and surface mass balance (SMB) (Table 13.5 in Church et al, 2013) and expert elicitation of total ice sheet mass loss from Bamber and Aspinall (2013). As in AR5, ice sheet SMB contributions are represented as being dependent on the forcing scenario, while ice sheet dynamics are not. Here, we use AR5's AIS and GIS SMB contributions from RCP2.6 for both the 1.5 °C and 2.0 °C GMST scenarios and the RCP4.5 projection for the 2.5 °C GMST scenario (Table 13.5 in Church et al, 2013). A spatiotemporal Gaussian process regression model is used to estimate the long-term contribution from non-climatic factors such as tectonics and GIA. To generate probability distributions of global mean and local sea level at a global network of tide gauge sites (Table S-1) for each GMST scenario, we use 10,000 Latin hypercube samples of probability distributions of individual sea level component contributions.

2.1.1 Approximating Global Temperature Stabilization with RCPs

The RCP-driven experiments in the CMIP5 archive are not designed to inform the assessment of climate impacts from incremental temperature changes. As such, we construct alternative ensembles for 1.5 °C, 2.0 °C, and 2.5 °C scenarios using CMIP5 output according to each AOGCM's 2100 GMST. Specifically, we create ensembles for 1.5 °C, 2.0 °C, and 2.5 °C scenarios with AOGCMs that have a 2100 GMST increase (19-yr running average) of 1.5 °C, 2.0 °C, and 2.5 °C (± 0.25 °C) relative to 1875–1900. Selection of the AOGCMs for each scenario ensemble are made irrespective of the AOGCM's RCP forcing. For model outputs that end in 2100, we extrapolate 19-yr running average GMST to 2100 based on the 2070–2090 trend. While we chose 2100 as the determining year for which AOGCMs are selected for each ensemble, it should be noted that Article 2 of the UNFCCC (UNFCCC, 1992) does not require that GMST stabilization be achieved within a particular time frame. The Paris Agreement likewise does not specify a timeframe for GMST stabilization, though its goal of brining net greenhouse gas (GHG) emissions to zero in the second half of the 21st century implies a similar time frame for stabilization. We make the assumption that AOGCM outputs that end at

2100 either stay within the range of the target ± 0.25 °C or fall below by any amount (i.e., undershoot). For AOGCMs that have GSMT output available after 2100, only those that undershoot the target are retained. However, we make an exception to this rule for the 2.5 °C scenario ensemble in order to include AOGCMs for generating post-2100 projections. For RCP4.5 and RCP6, GMST stabilization should not occur before 2150, when greenhouse gas concentrations stabilize (Meinshausen et al, 2011b) and so SLR projections after 2100 may not be representative of conditions under true GMST stabilization.

The GMST trajectories and GMSL contributions from TE and glacial ice from selected CMIP5 models that are binned into 1.5 °C, 2.0 °C, and 2.5 °C GMST categories are shown in Figs. 1 and S-2, respectively. For consistency with the K14 framework, which models 19-yr running averages of SLR relative to 2000, GMST is anomalized to 1991–2009 and then shifted upward by 0.72 °C to account for warming since 1875–1900 (Hansen et al, 2010; GISSTEMP Team, 2017). Table S-2 lists the AOGCMs employed in each GMST scenario ensemble and the sea-level components used. Given the paucity of CMIP5 output after 2100, the range of TE and GIC contributions to SLR in the 22nd century is likely underestimated relative to the 21st century.

2.2 Global mean sea-level rise projections from a semi-empirical sea level model

We generate estimates for GMSL for 2000–2100 using the SESL model from Kopp et al (2016a) driven with both GMST trajectories from CMIP5 models (Fig. 1) and GMST trajectories from the reduced-complexity climate model MAGICC6 (Meinshausen et al, 2011a, as employed in Rasmussen et al, 2016) for 2100 GMST targets of 1.5 °C, 2.0 °C, and 2.5 °C (± 0.25 °C) (Fig. S-3). The MAGICC6 GSMT trajectories are selected from all RCP-grouped projections using the same criteria as in Section 2.1.1. The SESL model is calibrated to the Common Era temperature reconstruction from Mann et al (2009) and the sea level reconstruction of Kopp et al (2016a). The historical statistical relationship between temperature and the rate of sea-level change is assumed to be constant; not included are nonlinear physical processes or critical threshold events that could substantially contribute to SLR, such as ice sheet collapse (Kopp et al, 2016b; Levermann et al, 2013). Threshold behavior is partially incorporated in the K14 framework through expert assessments of future ice sheet melt contributions (Bamber and Aspinall, 2013), which may be one reason why the K14 framework produces higher estimates in the upper tail of the SLR probability distribution for 2100.

2.3 Flood frequency estimation

2.3.1 Historic flood return levels

Extreme value theory is used with tide gauge observations to estimate the return levels of flood events of a given height, including those that occur less often, on average, than the length of the observational record (Coles, 2001b,a). Following Tebaldi et al (2012) and Buchanan et al (2016, 2017), we employ a generalized Pareto distribution (GPD) and a peaks-over-threshold approach to estimate the return periods of historical flood events at tide gauges. The GPD describes the probability of a given flood height conditional on an exceedance of the GPD threshold. Here, we use as the threshold the 99th percentile of daily maximum sea levels, which is generally both above the highest seasonal tide and balances the bias-variance trade-off in the GPD parameter estimation[1] (Tebaldi et al, 2012). The number of annual exceedances of the GPD threshold is assumed to be Poisson distributed with mean λ. The GPD parameters are estimated using the method of maximum likelihood with tide gauge observations referenced to Mean Higher High Water (MHHW)[2] above the 99th percentile in each tide gauge's record (*see Supporting Information*). Uncertainty in the GPD parameters is calculated from their covariance and is sampled using Latin hypercube sampling

[1] If too low of a GPD threshold is chosen, more observations than those exclusively in the tail of the GPD distribution might end up being included in the parameter calculation, causing bias. If too high of a GPD threshold is chosen, then too few observations may be incorporated in the estimation of distribution parameters leading to greater variance, relative to a case that uses more observations.

[2] Here defined as the average level of high tide over the last 19-years in each tide gauge record, which is different from the current U.S. National Tidal Datum Epoch of 1983–2001.

of a 1000 normally distributed GPD parameter pairs. For a given tide gauge, the annual expected number of exceedances of flood level z is given by $N(z)$:

$$N(z) = \begin{cases} \lambda \left(1 + \frac{\xi(z-\mu)}{\sigma}\right)^{-\frac{1}{\xi}} & \text{for } \xi \neq 0 \\ \lambda \exp(-\frac{z-\mu}{\sigma}) & \text{for } \xi = 0 \end{cases} \quad (1)$$

where the shape parameter (ξ) governs the curvature and upward statistical limit of the flood return curve, the scale parameter (σ) characterizes the variability in the exceedances caused by the combination of tides and storm surges, and the location parameter (μ) is the threshold water-level above which return-levels are estimated with the GPD. Meteorological and hydrodynamic differences between sites gives rise to differences in the shape parameter (ξ). Flood frequency distributions with $\xi > 0$ are "heavy tailed", due to a high frequency of extreme flood events (e.g., tropical and extra-tropical cyclones). Distributions with $\xi < 0$ are "thin tailed" and have a statistical upper bound on extreme flood levels. Events that occur between λ and 182.6/year (i.e., exceeding MHHW half of the days per year) are modeled with a Gumbel distribution as they are outside of the domain of the GPD.

2.3.2 Flood frequency amplification factors

The amplification factor (AF) quantifies the increase in the expected frequency of historical flood events (e.g., the 100-yr flood) due to SLR (Buchanan et al, 2017; Hunter, 2012; Church et al, 2013). Due to variation in the local storm climate and hydrodynamics, the height of flood events are unique to each location (SI Fig. S-4). The calculation of the expected AF includes both the uncertainty in the estimates of the return periods of historical flood events and uncertainty in SLR projections. Following Buchanan et al (2017), we define the expected flood amplification factor AF(z) for flood events with height z as the ratio of the expected number of flood events after including uncertain SLR (δ) to the historical expected number of flood events:

$$\mathrm{AF}(z) = \frac{\mathrm{E}[N(z-\delta)]}{N(z)} \quad (2)$$

The flood AFs reported in this study should not be directly interpreted as changes in flood frequency. What constitutes a future flood event critically depends on the future level of coastal protection and adaptation efforts, both of which are unknown for most locations.

2.3.3 Assessment of population exposure

Following the methods used in Kopp et al (2017), we assess the current population exposed to permanent inundation from GMSL under each GMST stabilization scenario. We caution that this is not a measure of future population exposure, which will depend upon both population growth and the dynamic response of the population to rising sea levels, but is instead intended to provide a summary metric of the human significance of different sea levels. We use a 1-arcsec SRTM 3.0 digital elevation model from NASA (NASA JPL, 2013) that is referenced to local MHHW levels and this study's local SLR projection grids. Projected inundation areas are intersected with current national population (Bright et al, 2011) and national boundary data (Hijmans et al, 2012). For each GMST target, the population exposed is assessed at the 50th, 5th, and 95th percentile local SLR projection. Further details are provided in the Supplementary Information of Kopp et al (2017).

3 Results

3.1 Global mean sea-level rise

The GMSL projections for each GMST target from the K14 and SESL method are shown in Fig. 1 and are tabulated along with the component contributions in Table 1. For the K14 method, differences in median GMSL between 1.5 °C, 2.0 °C, and 2.5 °C GMST stabilization targets do not appear until after 2050, when the 1.5 °C scenario begins to separate from the 2.0 °C and 2.5 °C trajectories (Table 1). The median GMST

trajectories diverge earlier, around 2030 (Fig. S-3). This is consistent with the early to mid-century divergence in the radiative forcing pathways and this study's allocation of RCPs in the 1.5 °C (primarily RCP2.6), 2.0 °C (primarily RCP4.5), and 2.5 °C (primarily RCP4.5 and RCP6) scenarios (Table S-2). Median projections for 2100 GMSL under a 1.5 °C scenario are 47 cm, with a *likely* range (67% probability) of 35–63 cm. An additional 8–11 cm of median GMSL rise is found for the 2.0 °C and 2.5 °C GMST scenarios, 55 cm (*likely* 40–74 cm) and 58 cm (*likely* 44–75 cm), respectively. The sources of GMSL projection variance are shown in SI Fig. S-5. Using the same framework, Kopp et al (2014) found similar median 2100 GMSL projections under RCP2.6 and RCP4.5: 50 cm (*likely* 37–65 cm) and 59 cm (*likely* 45–77 cm), respectively.

Despite being warmer by a half-degree, the 2.5 °C scenario largely overlaps the GMSL probability distribution for the 2.0 °C scenario (Fig. 1). For all GMST scenarios considered, TE contributes the most to median 2100 GMSL, and we find weak correlation ($r^2 = 0.10$) between 2100 GMST and the corresponding TE contribution (Fig. S-6). The latter is due in part to variation in the transient climate response (TCR) and ocean heat uptake efficiency across CMIP5 models (Kuhlbrodt and Gregory, 2012; Raper et al, 2002). To test the sensitivity of model-RCP filtering to the choice of GMST stabilization, we additionally calculate GMSL under a 1.75 °C and 2.25 °C scenario. The median 2100 GMSL under the 1.75 °C scenario is 6 cm greater than the 1.5 °C scenario, and the 2.25 °C scenario is 1 cm less than the 2.0 °C scenario (Table S-3), suggesting that GMST scenarios that are primarily represented by only one RCP may be more sensitive to model filtering.

Agreement between central estimates from process-based and semi-empirical projections implies consistency with the observed statistical relationship between GMST and the rate of SLR used to calibrate the SESL model. Across scenarios, median 2100 GMSL projections from the SESL model driven with CMIP5 GMST trajectories are 6–7 cm lower than those from the K14 framework (Fig. 1 and Table 1), a difference that is less in magnitude to those between the K14 projections and Kopp et al (2016a) SESL projections for RCPs 2.6 and 4.5 (Kopp et al, 2016a, Table 2, showing median SESL projections of 38 cm and 51 cm for RCP2.6 and 4.5, vs. 50 and 59 cm for K14). The agreement between the processed-based and SESL projections is less when driven with the MAGICC GMST trajectories shown in SI Fig. S-3 (median projection differences of 8–11 cm; Table 1). Similarly, median estimates of 2100 GMSL for 1.5 °C and 2.0 °C scenarios from Schleussner et al (2016a) are 5–6 cm less than the projections using the K14 framework (Table 1). The SLR projections of Schleussner et al (2016a) are based on a method that scales SLR component contributions as a function of GMST and ocean heat uptake (Perrette et al, 2013).

3.2 Population inundation

Under the median projected GMSL for a 2.0 °C GMST stabilization, areas currently home to about 60 million people are at risk of being permanently submerged by 2150, including areas currently home to half a million inhabitants of United Nations defined Small Island Developing States (SIDS). By comparison, under the median projection for the 1.5 °C stabilization scenario, areas currently home to about 5 million people, including 40,000 in SID avoid inundation (Table 2). Aggregation of the SIDS can mask important risks. For instance, local SLR projections for 2150 under a 1.5 °C GMST stabilization place areas currently home to almost a quarter of the current population of the Marshall Islands at risk of being permanently submerged.

3.3 Amplification of flood events

We assess the effects of different GMST stabilizations on coastal flooding by highlighting four cities: 1) New York, New York, USA 2) San Juan, Puerto Rico, USA 3) Cruxhaven, Lower Saxony, Germany, and 4) Kushimoto, Wakayama, Japan (Fig. 2). Estimates of the current 10-, 100-, and 500-yr flood (10%, 1%, 0.2% probability per year) and the future flood amplification factor (AF) for all sites are provided in SI Tables S-4 to S-6. Under a 2.0 °C GMST stabilization, the 2100 median local SLR for New York City is 69 cm, relative to 2000 (*likely* 43–98 cm). In Fig. 2, median local SLR shifts the expected historic flood return curve to the right [i.e., $N(z)$, the heavy grey curve, becomes $N+SL_{50}$ 2.0 °C, the dashed green curve] and increases the expected annual number of current 10-yr floods (a flood with a height of 1.09 m above MHHW) from 0.1/year to ∼10/year. However, when both the uncertainty in the GPD fit and the SLR projections are considered in the calculation of the projected future flood return curve (i.e., N_e 2.0 °C; the heavy green

curve), the 10-yr flood amplification increases to 26/year (i.e., > 2/month). The discontinuities in the flood return curves demarcate the threshold where events are modeled with either a Gumbel distribution (from λ to 182.6 events per year) and with the GPD (Buchanan et al, 2016). GHG mitigation that stabilizes GMST at 1.5 °C reduces median local SLR at New York City to 55 cm (*likely* 35–78 cm), and reduces the number of expected annual 10-yr flood events by half (13/year). By 2150, the reduction in expected 10-yr flood events from the 2.0 °C to the 1.5 °C scenario is still roughly 50% (58/year vs. 97/year; Table S-1).

Sea-level rise will increase the frequency of all flood events, but some flood events will amplify more than others. While higher frequency events (i.e., the current 10-yr flood event) are expected to increase the most for New York City by 2100, San Juan is expected to experience greater increases in lower frequency floods (i.e., 500-yr events). Specifically, GMST stabilized at 2.0 °C is anticipated to produce 23 current 500-yr floods per year, on average (0.93 m above MHHW). If GMST warming is stabilized around 1.5 °C, the expected number of 500-yr floods is reduced by roughly half (12/year, on average). At higher levels of SLR, the most frequent flood events (e.g., the 10-yr flood) become driven by tidal events, as opposed to storm surges. By 2100, the 10-year flood is expected to occur almost every other day under all scenarios. For some sites, the AF for the 2.0 °C scenario may be greater than or equal to the AF for the 2.5 °C scenario. This can be observed for projections around the Baltic and North Sea where there is large uncertainty in the sign of the ocean dynamics contribution to local sea-level change between models. After 2100, the GMSL overlap between the 2.0 °C and 2.5 °C scenario projections leads to indistinguishable differences in flood projections for some locations (Fig. 1 and Table 1)

In Asia, under a 2.0 °C and 1.5 °C GMST stabilization, by 2100, Kushimoto is projected to have median local SLR of 77 cm (*likely* 57–102 cm) and 69 cm (*likely* 51–92 cm), respectively; increasing the current number of expected 100-yr floods for Kushimoto from 1/100 years, on average, to 104/year and 81/year, on average. Some locations are projected to have less local SLR compared to New York, San Juan, and Kushimoto, and therefore less flood amplification. By 2100, under both a 2.0 °C and 1.5 °C GMST stabilization, Cruxhaven is projected to have median local SLR increases of 54 cm (*likely* 29–83 cm) and 43 cm (*likely* 25–65 cm), respectively. Considering the entire projected probability distribution of SLR at Cruxhaven, the expected frequency of the current 500-yr flood event will become the future 100-yr flood.

We assess regional differences in 100-yr flood amplification between 2.0 °C and 1.5 °C GMST stabilization by binning ratios of 2.0 °C/1.5 °C expected AFs for 2050 and 2100 (Fig. 3). Bins on the right side of each graph become filled when there are flood benefits at stations from 1.5 °C over 2.0 °C GMST stabilization, while bins on the left side of each graph become filled when there are little or no benefits at stations from 1.5 °C GMST over 2.0 °C GMST stabilization. At mid-century, only a few sites indicate benefits from a 1.5 °C GMST stabilization that are greater than 50% reductions in 100-yr flood frequency as GMSL trajectories between scenarios have not appreciably separated from one another (Table 1). However, by 2100, larger flood benefits of 1.5 °C GMST stabilization are expected in Europe and the East and Gulf Coasts of the United States (U.S.), where flood amplification is reduced by roughly half. We find minimal flood benefits from achieving a 1.5 °C GMST stabilization rather than a 2.0 °C GMST stabilization for the West Coast of the U.S., the Pacific, and Indian Ocean regions (Fig. 3).

4 Discussion and Conclusions

The Paris Agreement seeks to stabilize GMST by limiting warming to "well below 2.0 °C above pre-industrial levels", but a recent literature review under the UNFCCC found the notion that "up to 2.0 °C of warming is considered safe, is inadequate" and that "limiting global warming to below 1.5 °C would come with several advantages" (UNFCCC, 2015b). However, given the geographic diversity of climate impacts from any GMST target, there cannot be an objective threshold that defines when all impacts reach unmanageable levels. The location-specific increases in the frequency of coastal floods is one such example. The selection of a GMST target has important implications for long-term GMSL rise and, consequently, coastal flooding. Assessing the distribution of impacts of incremental levels of warming on coastal flooding is of relevance to > 625 million people who currently reside in low-lying coastal areas (Neumann et al, 2015) and are vulnerable to current and future flood events. For countries without the economic and physical capacity to construct flood protection and flood-resilient infrastructure—including some recognized by the United Nations as Small Island Developing States—local SLR that results in permanent inundation and unmanageable flooding may

threaten their existence (Wong et al, 2014; Diaz, 2016). The only feasible option for maintaining habitability for these locations may be the management of GMST through international climate accords, like the Paris Agreement, that govern the long-term committed rise in GMSL.

Only considering changes to the mean local sea level, we find that roughly 5 million fewer inhabitants currently reside in lands that will be permanently submerged by 2150 under a 1.5 °C GMST stabilization compared to that of the 2.0 °C case, including 40,000 fewer inhabitants of SIDS (Table 2). The effects of GMST stabilization on coastal flooding varies greatly by region and by return level (e.g., the 10-yr versus the 100-yr flood, ect.). Globally, for the current 100-yr flood, we find that by 2100, the Eastern and Gulf coasts of the U.S. and Europe could benefit the most from a 1.5 °C GMST stabilization relative to a 2.0 °C GMST stabilization, with flood frequency amplification being reduced by about half. However, while fractional reductions may appear substantial in some cases, small absolute differences may warrant similar coastal flood risk management responses. For instance, for New York City, we estimate that the difference in the expected number of current 100-yr floods per year (0.01 events per year, on average) between a 2.0 °C to a 1.5 °C GMST stabilization is only 3 times per year to 2 times per year, on average (Fig. 2).

While these data could be used in support of local probabilistic risk management strategies that intend to reduce current and future exposure and vulnerability to extreme flood events, some caveats should be highlighted. First, while our projections carry probabilities, the probabilities should be viewed in light of the characterization of the uncertainty of each sea level component. The true probability distribution of some sea level components may be imperfectly sampled. Second, changes to storm frequency and severity as well as effects from waves could significantly influence future flood events (e.g., Reed et al, 2015; Hatzikyriakou and Lin, 2017). In this study, wave effects are not considered, and we assume that the frequency of storm arrivals and their intensity will remain constant—and thus the Poisson and GPD scale and shape parameters. Modifications could be made to encompass changes in these parameters with time (Emanuel, 2013; Knutson et al, 2010). Lastly, these projections are for specific tide gauge locations and they may not be representative of the greater vicinity in which they are located.

The selection of the level at which to stabilize the GMST in the coming years will determine the committed amounts of future GMSL (Clark et al, 2016; Levermann et al, 2013). Our projected coastal flood impacts through the end of the 22nd century should be placed in the context of longer timeframes. Stabilization of GMST does not imply stabilization of GMSL. Regardless of the mitigation scenario chosen, GMSL rise due to TE is expected to continue for centuries to millennia. Additionally, some studies suggest that sustained GMST warming above given thresholds, including those as low as 2 °C, will lead to a near-complete loss of the GIS over a millennium or more (Church et al, 2013, section 13.4.3). Coincident with continued GMSL rise will be further increases in the frequency of current flood events and an increasing number of currently inhabited areas that will be permanently submerged. A comprehensive approach to managing coastal flood risks would take into account changes on these very long time frames.

Acknowledgements We thank XX anonymous reviewers and Carl-Friedrich Schleussner and colleagues at Climate Analytics (Berlin) for the helpful discussions. REK was supported in part by a grant from Rhodium Group (for whom he has previously worked as a consultant), as part of the Climate Impact Lab consortium and in part NSF grant ICER-1663807. We acknowledge the World Climate Research Programme's Working Group on Coupled Modeling, which is responsible for CMIP, and we thank the climate modeling groups (listed in Supporting Information Table S-2) for producing and making available their model output. For CMIP, the U.S. Department of Energy's Program for Climate Model Diagnosis and Intercomparison provides coordinating support and led development of software infrastructure in partnership with the Global Organization for Earth System Science Portals. Code for generating sea-level projections is available in the ProjectSL (https://github.com/bobkopp/ProjectSL), LocalizeSL (https://github.com/bobkopp/LocalizeSL), and SESL (https://github.com/bobkopp/SESL) repositories on Github. Code for generating flood projections is available in the XXXX (D.J. will upload) repository on Github. The statements, findings, conclusions, and recommendations are those of the authors and do not necessarily reflect the views of the funding agencies.

References

Bamber JL, Aspinall WP (2013) An expert judgement assessment of future sea level rise from the ice sheets. Nat Clim Chang 3(4):424–427, DOI 10.1038/nclimate1778, URL http://dx.doi.org/10.1038/nclimate1778

Bittermann K, Rahmstorf S, Kopp RE, Kemp AC (in rev) Global mean sea-level rise in a world agreed upon in Paris. Environ Res Lett

Bright EA, Coleman PR, Rose AN, Urban ML (2011) LandScan 2010, Data Set

Buchanan MK, Kopp RE, Oppenheimer M, Tebaldi C (2016) Allowances for evolving coastal flood risk under uncertain local sea-level rise. Climatic Change 137(3):347–362, DOI 10.1007/s10584-016-1664-7, URL https://doi.org/10.1007/s10584-016-1664-7

Buchanan MK, Oppenheimer M, Kopp RE (2017) Amplification of flood frequencies with local sea level rise and emerging flood regimes. Environ Res Lett 064009(12):7

Caldwell PC, Merrifield MA, Thompson PR (2015) Sea level measured by tide gauges from global oceans — the Joint Archive for Sea Level holdings (NCEI Accession 0019568). NOAA National Centers for Environmental Information Dataset

Church J, Clark P, Cazenave A, et al (2013) Sea Level Change. In: Stocker T, Qin D, Plattner GK, et al (eds) Clim. Chang. 2013 Phys. Sci. Basis. Contrib. Work. Gr. I to Fifth Assess. Rep. Intergov. Panel Clim. Chang., Cambridge University Press, Cambridge, UK and New York, NY, USA, chap 13

Clark PU, Shakun JD, Marcott SA, et al (2016) Consequences of twenty-first-century policy for multi-millennial climate and sea-level change. Nat Clim Chang 6(4):360–369, URL http://dx.doi.org/10.1038/nclimate2923http://10.0.4.14/nclimate2923http://www.nature.com/nclimate/journal/v6/n4/abs/nclimate2923.html{#}supplementary-information

Coles S (2001a) Ch. 3: Classical Extreme Value Theory and Models. Lecture Notes in Control and Information Sciences, Springer, URL https://books.google.com/books?id=2nugUEaKqFEC

Coles S (2001b) Ch. 4: Threshold Models. Lecture Notes in Control and Information Sciences, Springer, URL https://books.google.com/books?id=2nugUEaKqFEC

Diaz DB (2016) Estimating global damages from sea level rise with the coastal impact and adaptation model (ciam). Climatic Change 137(1):143–156, DOI 10.1007/s10584-016-1675-4, URL https://doi.org/10.1007/s10584-016-1675-4

Emanuel KA (2013) Downscaling CMIP5 climate models shows increased tropical cyclone activity over the 21st century. Proc Natl Acad Sci U S A 110(30):12,219–24, DOI 10.1073/pnas.1301293110, URL http://www.pubmedcentral.nih.gov/articlerender.fcgi?artid=3725040{&}tool=pmcentrez{&}rendertype=abstract

Farrell WE, Clark JA (1976) On postglacial sea level. Geophysical Journal of the Royal Astronomical Society 46(3):647–667, DOI 10.1111/j.1365-246X.1976.tb01252.x, URL http://dx.doi.org/10.1111/j.1365-246X.1976.tb01252.x

GISSTEMP Team (2017) GISS Surface Temperature Analysis (GISTEMP). URL https://data.giss.nasa.gov/gistemp/

Hansen J, Ruedy R, Sato M, Lo K (2010) Global surface temperature change. Reviews of Geophysics 48(4):n/a–n/a, DOI 10.1029/2010RG000345, URL http://dx.doi.org/10.1029/2010RG000345, rG4004

Hatzikyriakou A, Lin N (2017) Simulating storm surge waves for structural vulnerability estimation and flood hazard mapping. Natural Hazards 89(2):939–962, DOI 10.1007/s11069-017-3001-5, URL https://doi.org/10.1007/s11069-017-3001-5

Held IM, Winton M, Takahashi K, et al (2010) Probing the fast and slow components of global warming by returning abruptly to preindustrial forcing. Journal of Climate 23(9):2418–2427, DOI 10.1175/2009JCLI3466.1, URL https://doi.org/10.1175/2009JCLI3466.1, https://doi.org/10.1175/2009JCLI3466.1

Hijmans R, Kapoor J, Wieczorek J, et al (2012) GADM database of Global Administrative Areas 2.0, Data Set

Hsiang S, Kopp R, Jina A, et al (2017) Estimating economic damage from climate change in the united states. Science 356(6345):1362–1369, DOI 10.1126/science.aal4369, URL http://science.sciencemag.org/content/356/6345/1362, http://science.sciencemag.org/content/356/6345/1362.full.pdf

Hunter J (2012) A simple technique for estimating an allowance for uncertain sea-level rise. Clim Change 113(2):239–252, DOI 10.1007/s10584-011-0332-1

Jevrejeva S, Jackson LP, Riva REM, Grinsted A, Moore JC (2016) Coastal sea level rise with warming above 2 °C. Proceedings of the National Academy of Sciences 113(47):13,342–13,347, DOI 10.1073/pnas.1605312113

Knutson TR, McBride JL, Chan J, et al (2010) Tropical cyclones and climate change. DOI 10.1038/ngeo779

Kopp RE, Horton RM, Little CM, et al (2014) Probabilistic 21st and 22nd century sea-level projections at a global network of tide-gauge sites. Earth's Future pp 383–407, DOI 10.1002/2014EF000239.Abstract

Kopp RE, Bittermann K, Horton BP, et al (2016a) Temperature-driven global sea-level variability in the Common Era. Proceedings of the National Academy of Sciences 113(38)

Kopp RE, Shwom RL, Wagner G, Yuan J (2016b) Tipping elements and climate–economic shocks: Pathways toward integrated assessment. Earth's Future 4(8):346–372, DOI 10.1002/2016EF000362, URL http://dx.doi.org/10.1002/2016EF000362, 2016EF000362

Kopp RE, Deconto RM, Bader DA, et al (2017) Implications of ice-shelf hydrofracturing and ice-cliff collapse mechanisms for sea-level projections. arXiv pp 1–26, arXiv:1704.05597v1

Kuhlbrodt T, Gregory JM (2012) Ocean heat uptake and its consequences for the magnitude of sea level rise and climate change. Geophys Res Lett 39(17):1–6, DOI 10.1029/2012GL052952

Levermann A, Griesel A, Hofmann M, Montoya M, Rahmstorf S (2005) Dynamic sea level changes following changes in the thermohaline circulation. Climate Dynamics 24(4):347–354, DOI 10.1007/s00382-004-0505-y, URL https://doi.org/10.1007/s00382-004-0505-y

Levermann A, Clark PU, Marzeion B, et al (2013) The multimillennial sea-level commitment of global warming. Proceedings of the National Academy of Sciences 110(34), DOI 10.1073/pnas.1219414110

Mann ME, Zhang Z, Rutherford S, et al (2009) Global signatures and dynamical origins of the little ice age and medieval climate anomaly. Science 326(5957):1256–1260, DOI 10.1126/science.1177303, URL http://science.sciencemag.org/content/326/5957/1256, http://science.sciencemag.org/content/326/5957/1256.full.pdf

Marzeion B, Levermann A (2014) Loss of cultural world heritage and currently inhabited places to sea-level rise. Environmental Research Letters 9(3):034,001, URL http://stacks.iop.org/1748-9326/9/i=3/a=034001

Marzeion B, Jarosch aH, Hofer M (2012) Past and future sea-level change from the surface mass balance of glaciers. Cryosph 6(6):1295–1322, DOI 10.5194/tc-6-1295-2012, URL http://www.the-cryosphere.net/6/1295/2012/

Meinshausen M, Raper SCB, Wigley TML (2011a) Emulating coupled atmosphere-ocean and carbon cycle models with a simpler model, magicc6 – part 1: Model description and calibration. Atmospheric Chemistry and Physics 11(4):1417–1456, DOI 10.5194/acp-11-1417-2011, URL https://www.atmos-chem-phys.net/11/1417/2011/

Meinshausen M, Smith SJ, Calvin K, et al (2011b) The {RCP} greenhouse gas concentrations and their extensions from 1765 to 2300. Clim Change 109(1-2):213–241, DOI 10.1007/s10584-011-0156-z

Milne GA, Gehrels WR, Hughes CW, Tamisiea ME (2009) Identifying the causes of sea-level change. Nat Publ Gr 2(7):471–478, DOI 10.1038/ngeo544, URL http://dx.doi.org/10.1038/ngeo544

Mitchell D, AchutaRao K, Allen M, et al (2017) Half a degree additional warming, prognosis and projected impacts (happi): background and experimental design. Geoscientific Model Development 10(2):571–583, DOI 10.5194/gmd-10-571-2017, URL https://www.geosci-model-dev.net/10/571/2017/

Mitrovica JX, Gomez N, Morrow E, et al (2011) On the robustness of predictions of sea level fingerprints. Geophys J Int (187):729–742, DOI 10.1111/j.1365-246X.2011.05090.x

Mohammed K, Islam AS, Islam GT, et al (2017) Extreme flows and water availability of the brahmaputra river under 1.5 and 2 °c global warming scenarios. Climatic Change DOI 10.1007/s10584-017-2073-2, URL https://doi.org/10.1007/s10584-017-2073-2

Moss RH, Edmonds Ja, Hibbard Ka, et al (2010) The next generation of scenarios for climate change research and assessment. Nature 463(7282):747–56, DOI 10.1038/nature08823, URL http://www.ncbi.nlm.nih.gov/pubmed/20148028

NASA JPL (2013) NASA Shuttle Radar Topography Mission Global 1 arc second [Data set], NASA LP DAAC

Neumann B, Vafeidis AT, Zimmermann J, Nicholls RJ (2015) Future coastal population growth and exposure to sea-level rise and coastal flooding - A global assessment. PLoS One 10(3), DOI 10.1371/journal.pone.0118571

Perrette M, Landerer F, Riva R, Frieler K, Meinshausen M (2013) A scaling approach to project regional sea level rise and its uncertainties. Earth System Dynamics 4(1):11–29, DOI 10.5194/esd-4-11-2013, URL https://www.earth-syst-dynam.net/4/11/2013/

Rahmstorf S (2007) A semi-empirical approach to projecting future sea-level rise. Science 315(5810):368–370, DOI 10.1126/science.1135456, URL http://science.sciencemag.org/content/315/5810/368, http://science.sciencemag.org/content/315/5810/368.full.pdf

Rahmstorf S, Perrette M, Vermeer M (2012) Testing the robustness of semi-empirical sea level projections. Climate Dynamics 39(3):861–875, DOI 10.1007/s00382-011-1226-7, URL https://doi.org/10.

1007/s00382-011-1226-7

Raper SCB, Gregory JM, Stouffer RJ (2002) The Role of Climate Sensitivity and Ocean Heat Uptake on AOGCM Transient Temperature Response. Journal of Climate 15(1):124–130, DOI 10.1175/1520-0442(2002)015<0124:TROCSA>2.0.CO;2, URL https://doi.org/10.1175/1520-0442(2002)015<0124:TROCSA>2.0.CO;2, https://doi.org/10.1175/1520-0442(2002)015<0124:TROCSA>2.0.CO;2

Rasmussen DJ, Meinshausen M, Kopp RE (2016) Probability-weighted ensembles of u.s. county-level climate projections for climate risk analysis. Journal of Applied Meteorology and Climatology 55(10):2301–2322, DOI 10.1175/JAMC-D-15-0302.1, URL https://doi.org/10.1175/JAMC-D-15-0302.1, https://doi.org/10.1175/JAMC-D-15-0302.1

Reed AJ, Mann ME, Emanuel KA, et al (2015) Increased threat of tropical cyclones and coastal flooding to new york city during the anthropogenic era. Proceedings of the National Academy of Sciences 112(41):12,610–12,615, DOI 10.1073/pnas.1513127112, URL http://www.pnas.org/content/112/41/12610.abstract, http://www.pnas.org/content/112/41/12610.full.pdf

Schaeffer M, Hare W, Rahmstorf S, Vermeer M (2012) Long-term sea-level rise implied by 1.5 °C and 2 °C warming levels. Proceedings of the National Academy of Sciences 2(December 2012):867–870, DOI 10.1038/nclimate1584

Schleussner Cf, Lissner TK, Fischer EM, et al (2016a) Differential climate impacts for policy-relevant limits to global warming: the case of 1.5 °C and 2 °C. Earth System Dynamics 7(2):327–351, DOI 10.5194/esd-7-327-2016

Schleussner CF, Rogelj J, Schaeffer M, et al (2016b) Science and policy characteristics of the paris agreement temperature goal. Nature Clim Change 6(9):827–835, URL http://dx.doi.org/10.1038/nclimate3096

Strauss BH, Kulp S, Levermann A (2015) Mapping Choices: Carbon, Climate, and Rising Seas, Our Global Legacy. Climate Central Research Report pp 1–38

Sweet WV, Park J (2014) From the extreme to the mean: Acceleration and tipping points of coastal inundation from sea level rise. Earth's Future 2(12):579–600, DOI 10.1002/2014EF000272, URL http://dx.doi.org/10.1002/2014EF000272, 2014EF000272

Taylor KE, Stouffer RJ, Meehl GA (2012) An overview of cmip5 and the experiment design. Bulletin of the American Meteorological Society 93(4):485–498, DOI 10.1175/BAMS-D-11-00094.1, URL https://doi.org/10.1175/BAMS-D-11-00094.1, https://doi.org/10.1175/BAMS-D-11-00094.1

Tebaldi C, Strauss BH, Zervas CE (2012) Modelling sea level rise impacts on storm surges along US coasts. Environ Res Lett 7(1):014,032, DOI 10.1088/1748-9326/7/1/014032, URL http://stacks.iop.org/1748-9326/7/i=1/a=014032?key=crossref.99de1b370a3cea938a4cc90baa21719e

UNFCCC (1992) The United Nations Framework Convention on Climate Change, UNFCCC

UNFCCC (2015a) Report of the Conference of the Parties on its twenty-first session, held in Paris from 30 November to 13 December 2015, UNFCCC

UNFCCC (2015b) Report on the structured expert dialogue on the 2013–2015 review, UNFCCC

Vermeer M, Rahmstorf S (2009) Global sea level linked to global temperature. Proceedings of the National Academy of Sciences 106(51):21,527–21,532, DOI 10.1073/pnas.0907765106, URL http://www.pnas.org/content/106/51/21527.abstract, http://www.pnas.org/content/106/51/21527.full.pdf

van Vuuren DP, Edmonds J, Kainuma M, et al (2011) The representative concentration pathways: an overview. Climatic Change 109(1):5, DOI 10.1007/s10584-011-0148-z, URL https://doi.org/10.1007/s10584-011-0148-z

Wong PP, Losada IJ, Gattuso JP, et al (2014) Coastal systems and low-lying areas, Cambridge University Press, Cambridge, United Kingdom and New York, NY, USA, pp 361–409

5 Figures

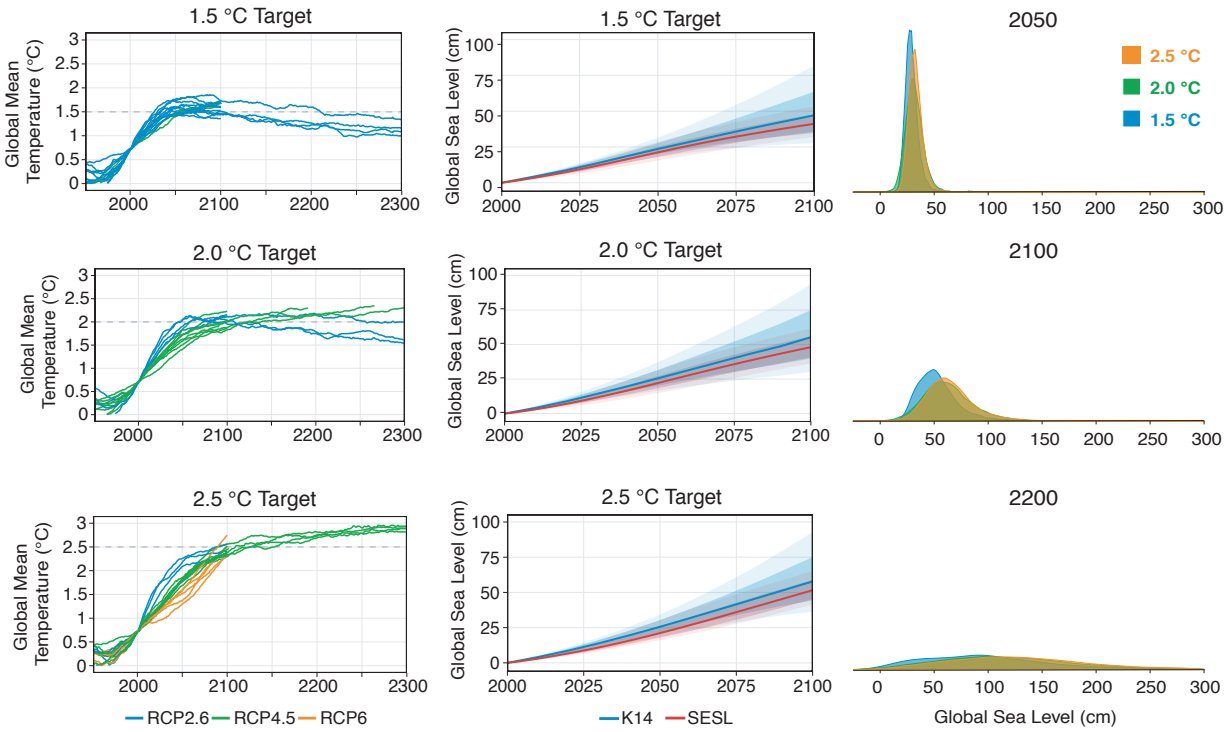


Fig. 1 Left Column: Global mean surface temperature (GMST) trajectories from CMIP5 models (1950–2300) that have a 19-year running average 2100 GMST of 1.5 °C, 2.0 °C, and 2.5 °C ± 0.25°C (relative to 1875–1900) (blue = RCP2.6, green = RCP4.5, orange = RCP6). GMST is anomalized to 1991–2009 and shifted up by 0.72°C to account for warming since 1875–1900 (Hansen et al, 2010; GISSTEMP Team, 2017). Table S-2 lists the models used for each temperature target. **Middle Column:** Global sea-level rise (cm; relative to 2000) from the methodology of Kopp et al (2014) (K14) (blue), using CMIP5 temperature trajectories from Left Column, and a semi-empirical global sea-level (SESL) model from Kopp et al (2016a) (red). Temperature trajectories that drive the SESL model are also shown in the Left Column. The thick line is the 50th percentile, heavy shading is the 17/83rd percentile, and light shading is the 5/95th percentile. **Right Column:** Probability distributions of projected 2050, 2100, and 2200 GMSL rise for GMST stabilization targets using the Kopp et al (2014) framework (blue = 1.5 °C, green = 2.0 °C, orange = 2.5 °C).

Table 1 GMSL projections. All values are cm above 2000 CE baseline. AIS = Antarctic Ice Sheet, GIS = Greenland Ice Sheet; TE = Thermal Expansion; GIC = Glacial Ice Melt; LWS = Land-Water Storage. K16: Semi-empirical sea level (SESL) model from Kopp et al (2016a) driven with global mean surface temperature (GMST) trajectories from MAGICC (see SI Fig. S-3) and CMIP5 GMST trajectories (see Fig. 1); J16: Jevrejeva et al (2016); S16: Schleussner et al (2016a); S12: Schaeffer et al (2012). *the estimate for Jevrejeva et al (2016) is not from 2100, rather it is upon reaching a median 2.0 °C GMST increase at mid-century in an RCP8.5 ensemble.

	1.5 °C			2.0 °C			2.5 °C		
cm	50	17–83	5–95	50	17–83	5–95	50	17–83	5–95
2100—Components									
AIS	6	-4–17	-8–35	6	-4–17	-8–35	5	-5–16	-9–33
GIS	6	4–12	3–17	6	4–12	3–17	9	4–15	2–23
TE	19	14–23	10–27	25	16–34	9–42	26	20–31	16–35
GIC	11	8–13	6–15	12	7–16	4–21	13	11–15	9–17
LWS	5	3–7	2–8	5	3–7	2–8	5	3–7	2–8
Total	47	35–64	28–82	55	40–75	30–94	58	44–75	36–93
Projections by year									
2050	24	20–28	18–32	25	20–32	17–37	26	21–30	19–34
2070	33	27–41	23–49	37	28–48	23–58	38	31–47	27–55
2100	47	35–64	28–82	55	40–75	30–94	58	44–75	36–93
2150	68	41–106	28–150	89	54–134	35–178	86	53–128	35–169
2200	91	41–159	19–240	120	64–197	32–277	117	61–192	30–269
Other projections for 2100									
K16[1]	38	33–43	30–47	45	39–52	35–58	54	47–62	42–68
K16[2]	41	36–48	32–53	48	41–56	36–62	51	45–59	41–65
J16*	–	–	–	22	–	15–33	–	–	–
S16	41	29–53	–	50	36–65	–	–	–	–
S12	77	–	54–99	80	–	56–105	–	–	–
Other projections for 2200									
S12	135	–	85–195	180	–	110–345	–	–	–

[1] SESL model driven with MAGICC6 GMST trajectories shown in SI Fig. S-3
[2] SESL model driven with CMIP5 GMST trajectories shown in Fig. 1

Table 2 Human population (in millions) currently residing on lands at risk of permanent inundation based on median (5–95th percentile) local SLR projections. Population estimates are from 2010. The top five countries with the most exposure in 2150 are included in the table as well as United Nations defined Small Island Developing States (SIDS).

Human population exposure under 2100 local SLR projections (millions)

Region	Total Pop.	1.5 °C	2.0 °C	2.5 °C
World	6,836.42	45.88 (31.87–68.83)	48.23 (31.99–78.38)	50.27 (33.15–77.28)
China	1,330.20	11.59 (5.87–20.22)	12.53 (5.98–21.69)	13.25 (6.12–22.93)
Vietnam	89.55	6.55 (4.55–9.85)	6.89 (4.58–10.44)	7.14 (4.65–11.07)
Japan	126.66	4.43 (3.82–5.54)	4.59 (3.87–5.77)	4.69 (3.88–6.10)
Netherlands	16.78	4.71 (4.19–5.56)	4.86 (4.18–5.88)	4.84 (4.35–5.63)
Bangladesh	156.13	2.81 (1.98–4.29)	3.00 (2.06–4.66)	3.09 (2.12–4.92)
SIDS	62.08	0.40 (0.30–0.55)	0.42 (0.30–0.63)	0.43 (0.31–0.63)

Human population exposure under 2150 local SLR projections (millions)

Region	Total Pop.	1.5 °C	2.0 °C	2.5 °C
World	6,836.42	55.49 (32.45–111.58)	60.48 (32.83–133.88)	61.95 (33.72–127.07)
China	1,330.20	14.22 (5.72–30.54)	16.38 (5.84–35.28)	16.51 (5.69–36.73)
Vietnam	89.55	7.53 (4.46–14.99)	8.3 (4.50–16.61)	8.27 (4.52–16.62)
Japan	126.66	4.89 (3.82–5.54)	5.3 (3.87–5.77)	5.34 (3.88–6.10)
Netherlands	16.78	5.06 (4.19–5.56)	5.17 (4.18–5.88)	5.26 (4.35–5.63)
Bangladesh	156.13	4.43 (1.98–4.29)	4.98 (2.06–4.66)	4.98 (2.12–4.92)
SIDS	62.08	0.46 (0.28–0.90)	0.50 (0.29–1.11)	0.51 (0.30–1.01)

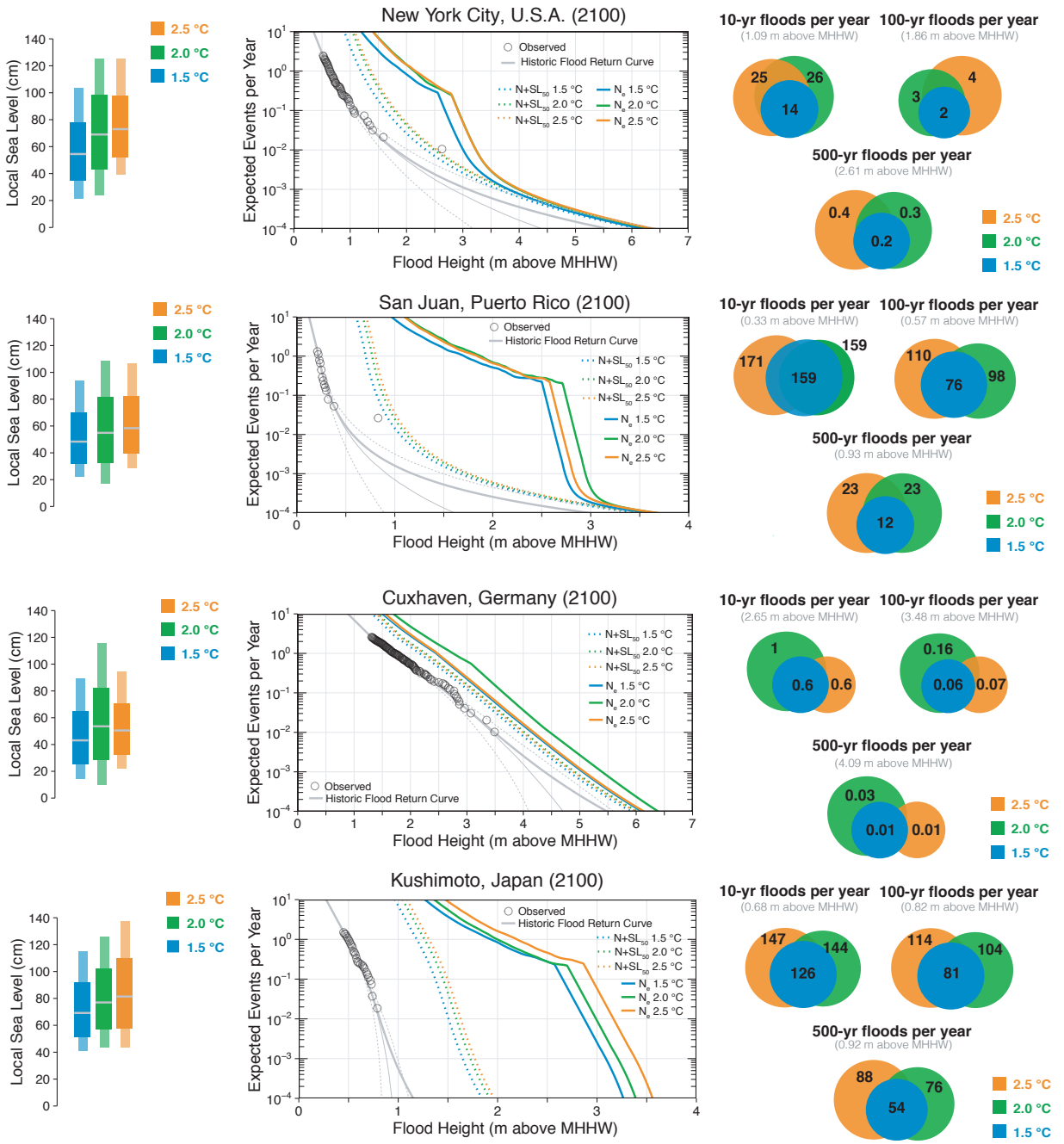


Fig. 2 Top Left: 2100 local sea-level rise (cm; relative to 2000) for New York City, U.S.A. under 1.5 °C (blue), 2.0 °C (green), and 2.5 °C (orange) global mean surface temperature (GMST) stabilization. Grey bars are median, heavy colors are 17/83 percentile and light shading is 5/95 percentile. **Top Middle:** Flood return curves for New York City indicating the relationship between the number of expected flood events $N(z)$ and flood level (z) for different GMST stabilizations (blue = 1.5 °C, green = 2.0 °C, orange = 2.5°C) and SLR assumptions for the year 2100. N denotes the historic flood return curve (heavy grey line), grey circles are historical flood events, thin grey lines are the 17/50/83 percentiles of the GPD parameter uncertainty range, respectively. Median SLR in 2100 for each GMST stabilization are depicted by $N + \mathrm{SL}_{50}$ curves, and the expected flood return levels are depicted as N_e. **Top Right:** The expected flood amplification factor (AF) for New York City for 10, 100, and 500-yr flood events for 2100 under a 1.5 °C (blue), 2.0 °C (green), and 2.5 °C (orange) GMST stabilization. **Second Row:** As for Top Row, but for San Juan, Puerto Rico. **Third Row:** As for Top Row, but for Cruxhaven, Germany. **Fourth Row:** As for Top Row, but for Kushimoto, Japan.

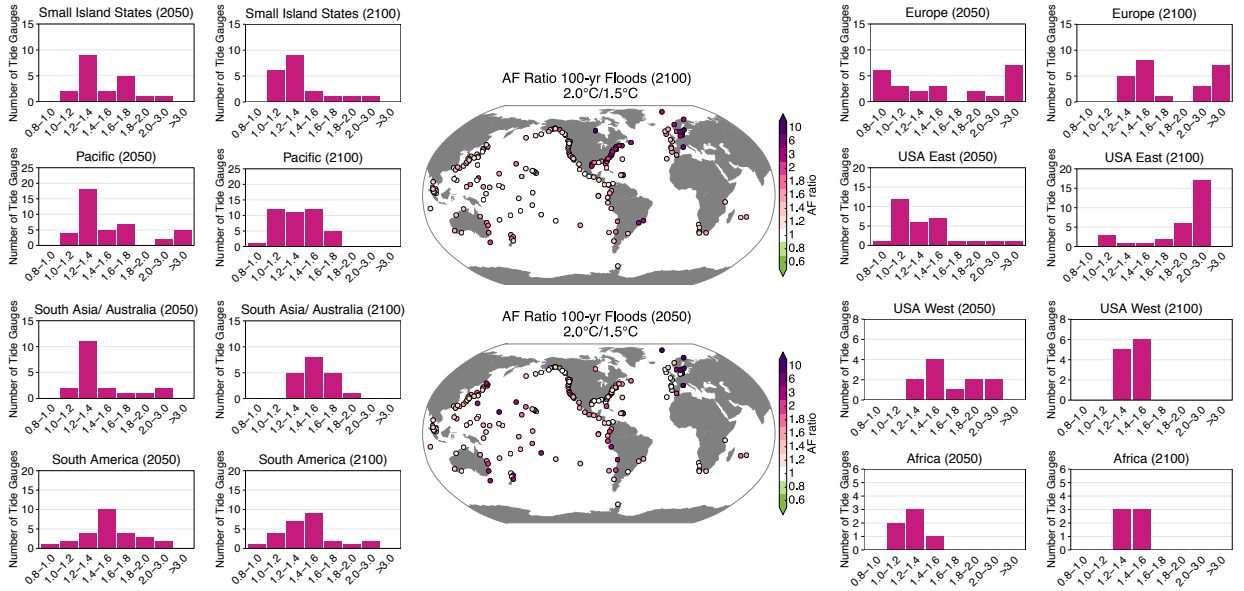


Fig. 3 Maps: The ratio of expected flood amplification factors (AFs) for 100-yr flood events between a 1.5 °C and 2.0 °C global mean surface temperature (GMST) stabilization target for the years 2050 and 2100. Larger 2.0 °C/1.5 °C AF ratios indicate locations where coastal flood benefits are greater from 1.5 °C GMST stabilization, relative to a 2.0 °C GMST stabilization. **Histograms:** Binned ratios of 2.0 °C/1.5 °C expected AFs for the 100-yr flood event for 2050 and 2100. "Small Island States" are Small Island Developing States defined by the United Nations. The list of sites included in each region are given in Table S-1.

Supplementary Information

S-1 Preparation of tide gauge data for extreme value analysis

Tide gauge observations are prepared as the basis for extreme value analysis following the methods of Tebaldi et al (2012). First, daily maximum tide gauge values are calculated from the "Research Quality" hourly observations from the University of Hawaii Sea Level Center (retrieved from uhslc.soest.hawaii.edu, June 2017; Caldwell et al, 2015). Only tide gauge locations with record lengths $\geq$ 30 years and $\geq$ 80 percent data completion are considered. A list of tide gauges and their record lengths is provided in the Table S-1. The impact of day-to-day weather, astronomical tides and seasonal cycles on sea level is isolated by removing sea level change over the tide gauge record. Monthly-mean sea levels over the tide gauge record are used to linearly de-trend the daily maximum observations. Mean higher high water (MHHW) at each tide gauge is estimated using the average of the daily maximum tide gauge observations over the most recent 19-year period. While the MHHW calculation approach differs from the current U.S. standard (which is defined over the National Tidal Datum Epoch of 1983–2001), it is taken after de-trending of the time series and therefore should be close to stationary. Each de-trended tide gauge series is then referenced to its own MHHW level. Finally, at each tide gauge the daily observations above the 99th percentile are de-clustered to separate multiple observations made during the same extreme flood event and so that each observation is independent of one another. The 99th percentile is used as it is generally above the highest seasonal tide and it balances the bias-variance trade-off in the GPD parameter estimation. If too low of a GPD threshold is chosen, more observations than those exclusively in the tail of the GPD distribution might end up being included in the parameter calculation, causing bias. If too high of a GPD threshold is chosen, then too few observations may be incorporated in the estimation of distribution parameters leading to greater variance, relative to a case that uses more observations.

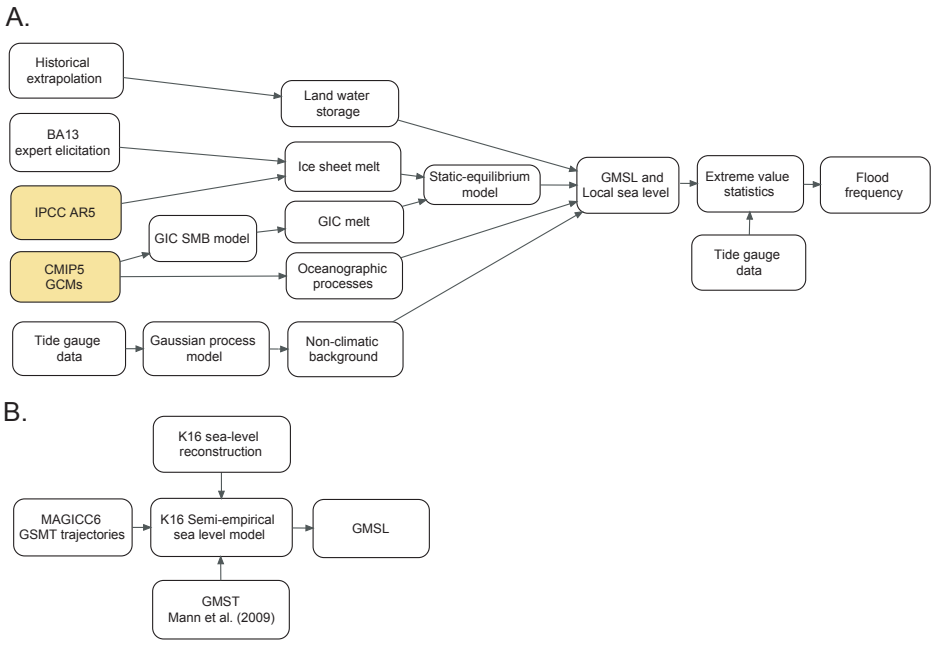


Fig. S-1 Top: Logical flow of sources of information used in local sea-level projections and flood frequency return curves. GCMs are global climate models; GIC is glacial ice contribution; SMB is surface mass balance; GMT is global mean temperature; GMSL is global mean sea level; BA13 is Bamber and Aspinall, 2013; K16 is Kopp et al, 2016a. Orange shades indicate where RCP and model grouping occurs (see Table S-2). **Bottom:** Logical flow of sources of information used to construct semi-empirical sea level GMSL projections.

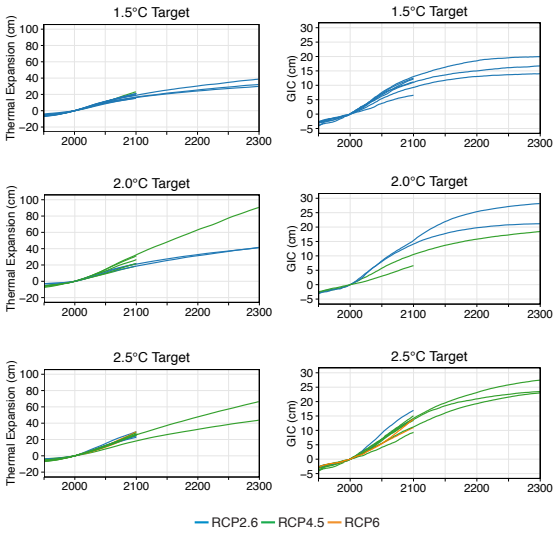


Fig. S-2 Left Column: Thermal expansion contribution to global mean sea-level (GMSL) rise (cm; relative to 2000) from CMIP5 models that have been smoothed and corrected for model drift for global mean surface temperature stabilization targets of 1.5 °C, 2.0 °C, and 2.5 °C (blue = RCP2.6, green = RCP4.5, orange = RCP6). **Right Column:** As for Left Column, but for the glacial ice contribution (GIC) to GMSL rise (cm; relative to 2000) using the model from Marzeion et al (2012). Table S-2 lists the models used for each temperature target.

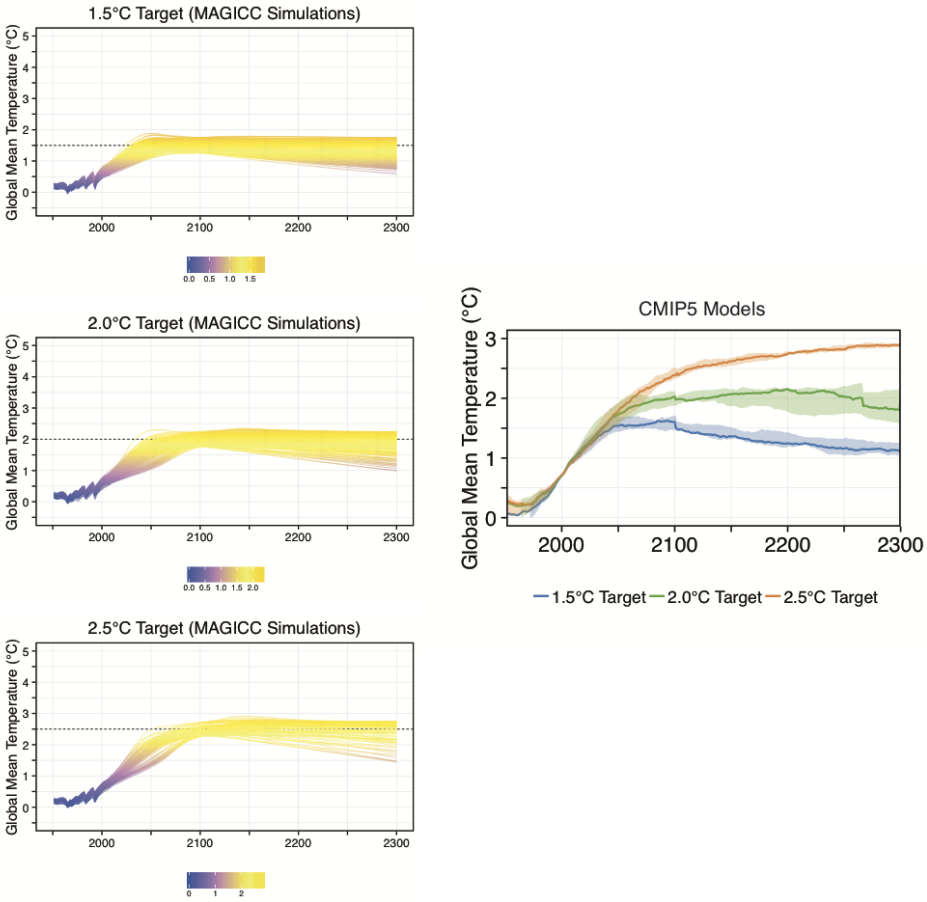


Fig. S-3 Left: Global mean temperature trajectories from MAGICC6 for 1.5°C, 2.0°C, and 2.5°C temperature targets at 2100. Temperatures are relative to 1875–1900. **Right:** Global mean surface temperature (GMST) trajectories from CMIP5 models (1950–2300) that have a 2100 GMST of 1.5 °C, 2.0 °C, and 2.5 °C ± 0.25°C (relative to 1875–1900). GMST is anomalized to 1991–2009 and shifted up by 0.72°C to account for warming since 1875–1900 (Hansen et al, 2010; GISSTEMP Team, 2017). Solid line is the 50th percentile and light shading is the 17th/83rd range.

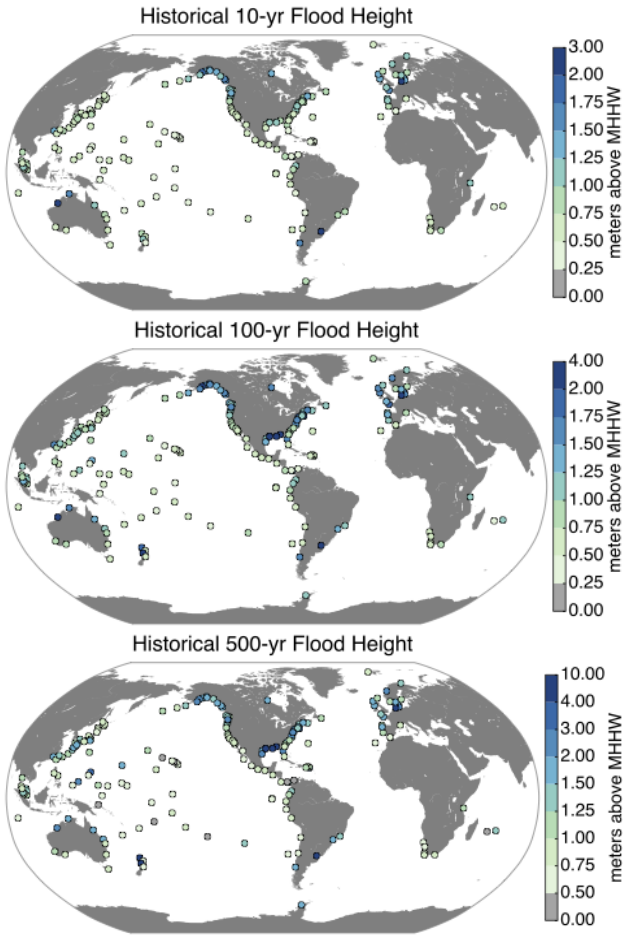


Fig. S-4 Historical flood height [meters above mean higher high water (MHHW)] of floods with return periods of 10-, 100-, and 500-years.

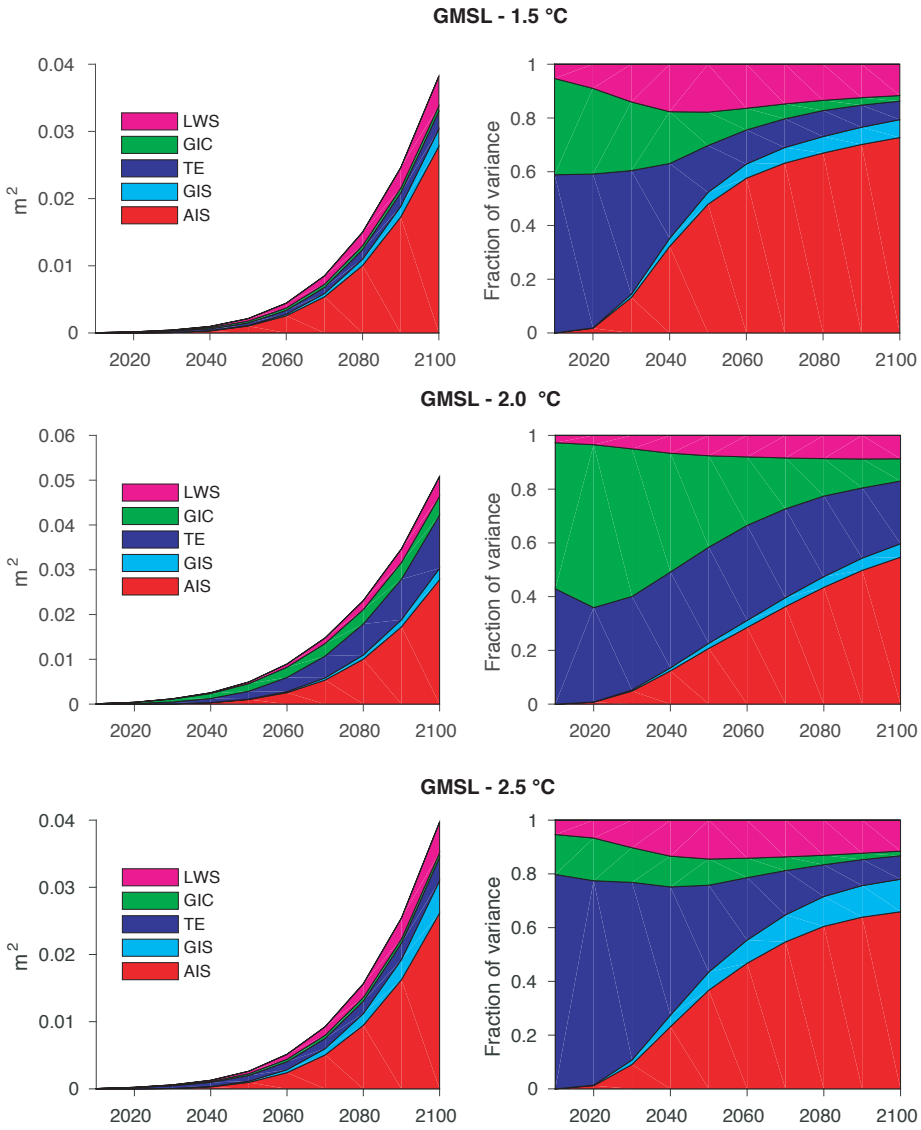


Fig. S-5 Global mean sea level (GMSL) sources of variance in raw and fractional terms in 1.5 °C, 2.0 °C, and 2.5 °C global mean surface temperature stabilization scenarios. AIS: Antarctic ice sheet, GIS: Greenland ice sheet, TE: thermal expansion, GIC: glaciers and ice caps, LWS: land water storage

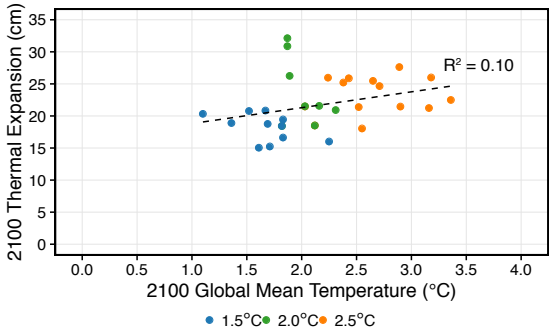


Fig. S-6 Relationship between 2100 global mean thermal expansion contribution to sea-level rise (i.e., 'zostoga') (cm) and the 19-yr running average of global mean surface temperature (GMST) for 2100 from CMIP5 model output (°C, relative to 1875–1900) under 1.5 °C (blue), 2.0 °C (green), and 2.5 °C (orange) GMST stabilization scenarios. Black dotted line is the linear fit across all temperature scenarios and all models.

Table S-1: List of tide gauges used from the University of Hawaii Sea Level Center and their record lengths.

Site	Country	Region	Lat	Lon	UHawaii ID	Start	End	Length (yrs)
Buenos Aires	Argentina	South America	-34.67	-58.50	285a	1905	1961	57
Fort Denison	Australia	South Asia/ Australia	-33.90	151.32	333a	1965	2015	51
Bundaberg	Australia	South Asia/ Australia	-24.77	152.50	332a	1984	2015	32
Brisbane	Australia	South Asia/ Australia	-27.37	153.17	331a	1984	2015	32
Spring Bay	Australia	South Asia/ Australia	-42.67	148.07	335a	1985	2015	31
Townsville	Australia	South Asia/ Australia	-19.25	146.83	334a	1984	2013	30
Broome	Australia	South Asia/ Australia	-18.02	122.23	166a	1986	2015	30
Cocos	Australia	South Asia/ Australia	-12.12	96.97	171a	1985	2015	31
Darwin	Australia	South Asia/ Australia	-12.52	130.97	168a	1984	2015	32
Esperance	Australia	South Asia/ Australia	-33.90	122.02	176a	1985	2015	31
Fremantle	Australia	South Asia/ Australia	-32.05	115.73	175a	1984	2015	32
Cananeia	Brazil	South America	-25.02	-48.00	281a	1954	2006	53
Ilha Fiscal, RJ	Brazil	South America	-23.02	-43.30	280a	1963	2012	50
Victoria, BC	Canada	Canada	48.50	-123.40	543a	1909	2014	106
Prince Rupert	Canada	Canada	54.32	-130.38	540a	1924	2014	91
Tofino	Canada	Canada	49.18	-126.03	542a	1930	2014	85
St. John's-A	Canada	Canada	47.57	-52.70	276a	1952	1989	38
Halifax	Canada	Canada	44.67	-63.58	275a	1899	2014	116
Churchill	Canada	Canada	58.77	-94.18	274a	1961	2012	52
Puerto Montt	Chile	South America	-41.50	-73.07	684a	1980	2014	35
Juan Fernandez-B	Chile	South America	-33.67	-78.95	021b	1985	2014	30
Antofagasta	Chile	South America	-23.68	-70.45	080a	1945	2014	70
Easter-C	Chile	South America	-27.20	-109.50	022c	1970	2014	45
Valparaiso	Chile	South America	-33.12	-71.72	081a	1944	2014	71
Xiamen	China	Pacific	24.45	118.07	376a	1954	1997	44
Buenaventura	Colombia	South America	3.95	-77.17	085a	1953	2014	62
Tumaco	Colombia	South America	1.82	-78.85	303a	1951	2014	64
Cartagena	Colombia	South America	10.38	-75.53	265a	1951	1993	43
Penrhyn	Cook Islands	SIDS	-9.07	-158.08	024a	1977	2015	39
Quepos-A	Costa Rica	South America	9.40	-84.17	087a	1961	1994	34
Hornbaek	Denmark	Europe	56.10	12.47	838a	1891	2012	122
Gedser	Denmark	Europe	54.57	11.93	837a	1891	2012	122
Baltra-B	Ecuador	South America	-0.47	-90.30	003b	1985	2015	31
Santa Cruz	Ecuador	South America	-0.80	-90.43	030a	1978	2015	38
La Libertad	Ecuador	South America	-2.20	-80.92	091a	1949	2015	67
Acajutla-A	El Salvador	South America	13.58	-89.83	082a	1962	2001	40
Chuuk	Fd. St. Micronesia	SIDS	7.45	151.85	054a	1956	1991	36
Kapingamarangi	Fd. St. Micronesia	SIDS	1.23	154.87	029a	1978	2015	38
Pohnpei-B	Fd. St. Micronesia	SIDS	7.02	158.33	001b	1974	2004	31
Yap-B	Fd. St. Micronesia	SIDS	9.58	138.23	008b	1969	2015	47
Suva-C	Fiji	SIDS	-18.27	178.52	018c	1972	2015	44
Noumea	France	Europe	-22.32	166.42	019a	1967	2015	49
Brest	France	Europe	48.38	-4.60	822a	1846	2014	169
Marseille	France	Europe	43.38	5.38	824a	1885	1988	104
Rikitea	French Polynesia	SIDS	-23.20	-134.98	016a	1969	2015	47
Papeete-B	French Polynesia	SIDS	-17.60	-149.57	015b	1975	2015	41
Cuxhaven	Germany	Europe	53.87	8.72	825a	1917	2014	98
Malin Head	Ireland	Europe	55.37	-7.33	834a	1958	2001	44
Hakodate	Japan	Pacific	41.78	140.72	364a	1964	2014	51
Hamada	Japan	Pacific	34.90	132.07	348a	1984	2014	31
Maisaka	Japan	Pacific	34.68	137.62	356a	1968	2014	47
Ishigaki	Japan	Pacific	24.33	124.15	365a	1969	2014	46
Naha	Japan	Pacific	26.22	127.67	355a	1966	2014	49
Toyama	Japan	Pacific	36.77	137.23	349a	1967	2014	48
Hosojima	Japan	Pacific	32.42	131.68	358a	1933	1975	43
Kushiro	Japan	Pacific	42.97	144.37	350a	1963	2014	52
Abashiri	Japan	Pacific	44.02	144.28	347a	1968	2014	47
Mera	Japan	Pacific	34.92	139.82	352a	1965	2014	50
Wakkanai	Japan	Pacific	45.40	141.68	360a	1967	2014	48
Chichijima	Japan	Pacific	27.10	142.18	047a	1975	2014	40
Nishinoomote	Japan	Pacific	30.75	131.07	363a	1965	2013	49
Naze	Japan	Pacific	28.52	129.60	359a	1957	2013	57
Hachinohe	Japan	Pacific	40.53	141.53	375a	1980	2011	32
Miyakejima	Japan	Pacific	34.07	139.62	357a	1964	2013	50

Continued on next page

Table S-1 – continued from previous page

Site	Country	Region	Lat	Lon	UHawaii ID	Start	End	Length (yrs)
Nakano Shima	Japan	Pacific	29.92	129.92	345a	1984	2013	30
Ofunato	Japan	Pacific	39.02	141.75	351a	1965	2014	50
Nagasaki	Japan	Pacific	32.73	129.87	362a	1985	2014	30
Aburatsu	Japan	Pacific	31.58	131.42	354a	1961	2014	54
Kushimoto	Japan	Pacific	33.48	135.77	353a	1961	2014	54
Cendering	Malaysia	South Asia/ Australia	5.40	103.22	320a	1984	2013	30
Johor Baharu	Malaysia	South Asia/ Australia	1.57	103.87	321a	1983	2013	31
Kuantan	Malaysia	South Asia/ Australia	4.05	103.55	322a	1983	2013	31
Keling	Malaysia	South Asia/ Australia	2.35	102.18	141a	1984	2013	30
Lumut	Malaysia	South Asia/ Australia	4.30	100.73	143a	1984	2013	30
Kelang	Malaysia	South Asia/ Australia	3.05	101.43	140a	1983	2013	31
Langkawi	Malaysia	South Asia/ Australia	6.90	99.80	142a	1985	2015	31
Penang	Malaysia	South Asia/ Australia	5.47	100.47	144a	1984	2013	30
Port Louis-C	Mauritius	SIDS	-20.20	57.60	103c	1986	2015	30
Rodrigues	Mauritius	SIDS	-19.68	63.43	105a	1986	2015	30
Manzanillo-A	Mexico	South America	19.08	-104.45	395a	1953	1982	30
Ensenada	Mexico	South America	31.85	-116.63	317a	1956	1991	36
Salina Cruz	Mexico	South America	16.25	-95.23	394a	1952	1983	32
Acapulco-A, Gro.	Mexico	South America	16.90	-100.02	316a	1952	1995	44
Cabo San Lucas	Mexico	South America	23.00	-109.98	034a	1973	2002	30
Guaymas	Mexico	South America	27.93	-110.90	397a	1953	1986	34
Saipan-B	N. Mariana Islands	SIDS	15.32	145.82	028b	1978	2015	38
Marsden Point	New Zealand	South Asia/ Australia	-35.83	174.50	398a	1975	2014	40
Tauranga	New Zealand	South Asia/ Australia	-37.65	176.18	073a	1984	2014	31
Taranaki	New Zealand	South Asia/ Australia	-39.05	174.03	076a	1984	2014	31
Wellington	New Zealand	South Asia/ Australia	-41.28	174.78	071a	1944	2014	71
Tregde	Norway	Europe	58.00	7.57	804a	1927	2008	82
Rorvik	Norway	Europe	64.87	11.25	803a	1969	2014	46
Ny-Alesund	Norway	Europe	78.93	11.95	823a	1976	2014	39
Vardo	Norway	Europe	70.33	31.10	805a	1979	2014	36
Balboa	Panama	South America	9.10	-79.63	302a	1907	2014	108
Cristobal	Panama	South America	9.40	-80.05	266a	1907	2014	108
Rabaul	Papua New Guinea	SIDS	-4.20	152.25	010a	1966	1997	32
Lobos de Afuera	Peru	South America	-6.93	-80.72	084a	1982	2014	33
Callao-B	Peru	South America	-12.08	-77.17	093b	1970	2015	46
Legaspi	Philippines	Pacific	13.25	123.83	371a	1984	2015	32
Manila	Philippines	Pacific	14.60	120.98	370a	1984	2015	32
Cascais	Portugal	Europe	38.77	-9.42	209a	1959	2005	47
Funchal-B	Portugal	Europe	32.73	-17.03	218b	1982	2013	32
Kanton-B	Rep. of Kiribati	SIDS	-2.90	-171.73	013b	1972	2012	41
Christmas-B	Rep. of Kiribati	SIDS	2.12	-157.52	011b	1974	2015	42
Majuro-A	Rep. of Marshall I	SIDS	7.17	171.43	005a	1968	1999	32
Kwajalein	Rep. of Marshall I	SIDS	8.73	167.73	055a	1946	2014	69
Malakal-B	Republic of Belau	SIDS	7.45	134.58	007b	1969	2015	47
Kaohsiung	Republic of China	Pacific	22.75	120.33	340a	1980	2014	35
Keelung	Republic of China	Pacific	25.22	121.85	341a	1980	2014	35
Luderitz	South Africa	Africa	-26.65	15.15	702a	1958	1995	38
Saldahna Bay	South Africa	Africa	-33.02	17.95	703a	1982	2011	30
Simon's Town	South Africa	Africa	-34.18	18.43	221a	1959	1999	41
Port Nolloth	South Africa	Africa	-29.25	16.87	701a	1958	1997	40
Port Elizabeth	South Africa	Africa	-34.05	25.75	184a	1978	2014	37
La Coruna	Spain	Europe	43.37	-8.40	830a	1943	2013	71
Ceuta	Spain	Europe	35.90	-5.32	207a	1944	2013	70
Vigo	Spain	Europe	42.23	-8.73	208a	1943	1990	48
Stockholm	Sweden	Europe	59.40	18.22	826a	1889	2014	126
Goteborg-Torsh.	Sweden	Europe	57.70	11.85	819a	1967	2014	48
Zanzibar	Tanzania	Africa	-6.20	39.25	151a	1984	2015	32
Ko Lak	Thailand	South Asia/ Australia	11.90	99.82	328a	1985	2015	31
Stornoway	United Kingdom	Europe	58.28	-6.43	295a	1976	2010	35
Lerwick	United Kingdom	Europe	60.20	-1.20	293a	1959	2010	52
Faraday	United Kingdom	Europe	-65.25	-64.27	700a	1978	2013	36
Gibraltar-A	United Kingdom	Europe	36.13	-5.35	289a	1961	1992	32
Bermuda-B	United Kingdom	Europe	32.43	-64.73	259b	1985	2014	30
Newlyn, Cornwall	United Kingdom	Europe	50.12	-5.62	294a	1915	2010	96
Seward-C, AK	USA	Canada	60.15	-149.52	560c	1967	2014	48
Ketchikan, AK	USA	Canada	55.33	-131.70	571a	1937	2014	78

Continued on next page

Table S-1 – continued from previous page

Site	Country	Region	Lat	Lon	UHawaii ID	Start	End	Length (yrs)
Valdez, AK	USA	Canada	61.20	-146.47	562a	1973	2014	42
Yakutat, AK	USA	Canada	59.68	-139.75	570a	1961	2014	54
Seldovia, AK	USA	Canada	59.50	-151.75	561a	1975	2014	40
Sitka, AK	USA	Canada	57.07	-135.42	559a	1938	2014	77
Sand Point, AK	USA	Canada	55.37	-160.52	574a	1973	2014	42
Dutch Harbor-B, AK	USA	Canada	54.00	-166.57	041b	1982	2014	33
Cordova-B, AK	USA	Canada	60.63	-145.78	583b	1964	2014	51
Kodiak Isl., AK	USA	Canada	57.87	-152.62	039a	1975	2014	40
Adak, AK	USA	Canada	51.98	-176.77	040a	1950	2014	65
San Francisco, CA	USA	USA West	37.87	-122.60	551a	1897	2014	118
San Diego, CA	USA	USA West	32.83	-117.23	569a	1906	2014	109
Los Angeles, CA	USA	USA West	33.75	-118.32	567a	1923	2014	92
Crescent City, CA	USA	USA West	41.85	-124.18	556a	1933	2014	82
Monterey, CA	USA	USA West	36.65	-121.93	555a	1973	2014	42
Port San Luis, CA	USA	USA West	35.27	-120.85	565a	1948	2014	67
Santa Monica, CA	USA	USA West	34.08	-118.50	578a	1973	2014	42
La Jolla, CA	USA	USA West	32.87	-117.32	554a	1924	2014	91
New London, CT	USA	USA East	41.40	-72.12	744a	1938	2014	77
Lewes, DE	USA	USA East	38.92	-75.15	747a	1957	2014	58
Fernandina Beach, FL	USA	USA East	30.72	-81.47	240a	1897	1930	34
St. Petersburg, FL	USA	USA East	27.85	-82.72	759a	1946	2014	69
Pensacola, FL	USA	USA East	30.43	-87.33	762a	1923	2014	92
Mayport, FL	USA	USA East	30.50	-81.57	753a	1928	2000	73
Limetree Bay, FL	USA	USA East	17.82	-64.78	254a	1982	2014	33
Key West, FL	USA	USA East	24.58	-81.88	242a	1913	2014	102
Fort Pulaski, GA	USA	USA East	32.03	-80.92	752a	1935	2014	80
Hilo, HI	USA	Pacific	19.73	-155.07	060a	1927	2014	88
French Frigate, HI	USA	Pacific	23.88	-166.33	014a	1974	2007	34
Kahului, HI	USA	Pacific	20.90	-156.47	059a	1950	2014	65
Mokuoloe, HI	USA	Pacific	21.43	-157.80	061a	1957	2014	58
Honolulu-B, HI	USA	Pacific	21.37	-157.87	057b	1905	2014	110
Nawiliwili, HI	USA	Pacific	21.97	-159.35	058a	1954	2014	61
Grand Isle, LA	USA	USA East	29.38	-90.02	765a	1980	2014	35
Woods Hole, MA	USA	USA East	41.58	-70.72	742a	1957	2014	58
Nantucket, MA	USA	USA East	41.30	-70.22	743a	1965	2014	50
Boston, MA	USA	USA East	42.40	-71.07	741a	1921	2014	94
Portland, ME	USA	USA East	43.72	-70.37	252a	1910	2014	105
Eastport, ME	USA	USA East	44.93	-67.00	740a	1929	2014	86
Duck Pier, NC	USA	USA East	36.18	-75.87	260a	1978	2014	37
Wilmington, NC	USA	USA East	34.32	-77.98	750a	1935	2014	80
Atlantic City, NJ	USA	USA East	39.40	-74.43	264a	1911	2014	104
Cape May, NJ	USA	USA East	38.98	-75.05	746a	1965	2014	50
Montauk, NY	USA	USA East	41.18	-72.05	279a	1959	2014	56
New York, NY	USA	USA East	40.70	-74.15	745a	1920	2014	95
Charleston, OR	USA	USA West	43.45	-124.37	575a	1978	2014	37
South Beach, OR	USA	USA West	44.70	-124.13	592a	1967	2014	48
Astoria, OR	USA	USA West	46.28	-123.77	572a	1925	2014	90
Newport, RI	USA	USA East	41.55	-71.42	253a	1930	2014	85
Charleston, SC	USA	USA East	32.92	-80.00	261a	1921	2014	94
Rockport, TX	USA	USA East	28.07	-97.17	769a	1944	2014	71
Port Isabel, TX	USA	USA East	26.15	-97.35	772a	1977	2014	38
Chesapeake BBT, VA	USA	USA East	36.97	-76.23	749a	1975	2014	40
Neah Bay, WA	USA	USA East	48.38	-124.62	558a	1934	2014	81
Willapa Bay, WA	USA	USA East	46.78	-124.10	564a	1972	2014	43
Galveston, Pier 21, TX	USA	USA East	29.40	-94.88	775a	1904	2014	111
Galveston, P. Pier, TX	USA	USA East	29.32	-94.85	767a	1957	2011	55
Apra Harbor, Guam	USA Trust	Pacific	13.43	144.65	053a	1948	2014	67
Wake	USA Trust	Pacific	19.28	166.62	051a	1950	2014	65
Johnston	USA Trust	Pacific	16.78	-169.65	052a	1947	2015	69
Midway	USA Trust	Pacific	28.22	-177.37	050a	1947	2014	68
Pago Pago	USA Trust	Pacific	-14.28	-170.68	056a	1948	2014	67
Charlotte Amalie, VI	USA Trust	SIDS	18.35	-64.95	255a	1978	2014	37
San Juan, PR	USA Trust	SIDS	18.55	-66.12	245a	1977	2014	38
Magueyes Island, PR	USA Trust	SIDS	18.02	-67.17	246a	1965	2014	50

Table S-2 Inventory of CMIP5 models and RCPs used for 1.5 °C, 2.0 °C, and 2.5 °C global mean surface temperature (GMST) stabilization targets. Information is given for the 19-yr running average 2100 GMST (°C; relative to 1875–1900) and the lengths of the GMST projections and the contributions to sea-level change from oceanographic processes and glacial ice (GIC; from Marzeion et al (2012)). 'Local Ocean' is the local sea surface height above the geoid (i.e., 'zos') and 'Thermal Expansion' refers to the contribution to the change in the global mean sea level due to thermal expansion (i.e.,'zostoga').

1.5 °C

Model	RCP	2100 GMST (°C)	GMST	Local Ocean	Thermal Expansion	GIC
bcc-csm1-1	RCP 2.6	1.51	23	23	23	23
BNU-ESM	RCP 2.6	1.62	21			
CCSM4	RCP 2.6	1.45	23	23	21	21
FIO-ESM	RCP 4.5	1.7	21	21		
GFDL-ESM2G	RCP 4.5	1.61	21	21		
HadGEM2-AO	RCP 2.6	1.74	21			
IPSL-CM5A-LR	RCP 2.6	1.74	23	23	23	23
IPSL-CM5A-MR	RCP 2.6	1.6	21	21	21	
MIROC5	RCP 2.6	1.62	21			21
MPI-ESM-LR	RCP 2.6	1.44	23	23	23	23
MPI-ESM-MR	RCP 2.6	1.36	21	21	21	
MRI-CGCM3	RCP 2.6	1.72	21	21	21	21
NorESM1-M	RCP 2.6	1.52	21	21	21	21
NorESM1-ME	RCP 2.6	1.67	21	21	21	

2.0 °C

Model	RCP	2100 GMST (°C)	GMST	Local Ocean	Thermal Expansion	GIC
bcc-csm1-1	RCP 4.5	2.21	23			23
bcc-csm1-1-m	RCP 4.5	2.13	21	21	21	
CanESM2	RCP 2.6	2.17	23	23	23	23
CESM1-BGC	RCP 4.5	2.24	21	21		
CESM1-CAM5	RCP 2.6	2.13	23			
CSIRO-MK3-6-0	RCP 2.6	2.04	21		21	
FGOALS-G2	RCP 4.5	2.01	23			
GFDL-ESM2M	RCP 4.5	1.84	22	21	21	
GISS-E2-H-CC	RCP 4.5	2.03	21			
GISS-E2-R	RCP 4.5	1.88	23	23	23	23
GISS-E2-R-CC	RCP 4.5	1.87	21	21	21	
HadGEM2-ES	RCP 2.6	1.97	23	23	23	23
inmcm4	RCP 4.5	2.04	21	21	21	21

2.5 °C

Model	RCP	2100 GMST (°C)	GMST	Local Ocean	Thermal Expansion	GIC
CCSM4	RCP 4.5	2.31	23	23	21	21
CNRM-CM5	RCP 4.5	2.56	23	23	23	23
FIO-ESM	RCP 6.0	2.34	21	21		
GFDL-CM3	RCP 2.6	2.57	21	21	21	21
GFDL-ESM2G	RCP 6.0	2.35	21	21	21	
GFDL-ESM2M	RCP 6.0	2.53	21	21	21	
GISS-E2-R	RCP 6.0	2.52	21	21	21	21
IPSL-CM5B-LR	RCP 4.5	2.37	21	21		
MIROC-ESM	RCP 2.6	2.32	21	21	21	21
MIROC-ESM-CHEM	RCP 2.6	2.42	21	21	21	
MIROC5	RCP 4.5	2.38	21		21	21
MPI-ESM-LR	RCP 4.5	2.38	23	23	23	23
MPI-ESM-MR	RCP 4.5	2.39	21	21	21	
MRI-CGCM3	RCP 4.5	2.51	21	21		21
NorESM1-M	RCP 6.0	2.74	21	21	21	23
NorESM1-M	RCP 4.5	2.33	23	23	21	
NorESM1-ME	RCP 4.5	2.44	21	21	21	

21 = to 2100, 22 = to 2200, 23 = to 2300

Table S-3 GMSL projections from a 1.75 °C and a 2.25 °C GMST scenario. All values are cm above 2000 CE baseline. AIS = Antarctic Ice Sheet, GIS = Greenland Ice Sheet; TE = Thermal Expansion; GIC = Glacial Ice Melt; LWS = Land-Water Storage.

	1.75°C			2.25°C		
cm	50	17–83	5–95	50	17–83	5–95
2100—Components						
AIS	6	-4–17	-8–35	6	-4–17	-8–35
GIS	6	4–12	3–17	6	4–12	3–17
TE	21	12–30	6–37	23	20–27	17–30
GIC	12	8–15	6–17	13	9–16	6–20
LWS	5	3–7	2–8	5	3–7	2–8
Total	51	36–70	27–90	54	41–70	34–90
Projections by year						
2050	25	20–30	17–34	25	21–30	18–34
2070	35	27–45	22–54	37	30–45	26–54
2100	51	36–70	27–90	54	41–70	34–90
2150	73	44–110	30–158	80	51–115	38–163
2200	98	46–164	21–252	107	55–172	30–260

Table S-4: Expected flood amplification factors (AF) for the 10-yr flood for 2050, 2100, and 2150 under 1.5°C, 2.0°C, and 2.5°C global mean surface temperature stabilization scenarios.

			10-yr Flood								
			2050			2100			2150		
Site	Region	Historical Height (m above MHHW)	AF 1.5°C	AF 2.0°C	AF 2.5°C	AF 1.5°C	AF 2.0°C	AF 2.5°C	AF 1.5°C	AF 2.0°C	AF 2.5°C
Buenos Aires	Argentina	2.15	2.1	2.3	2.3	8.1	12.6	13.8	57.3	100.5	95.5
Fort Denison	Australia	0.63	27.7	57.0	48.6	460.2	746.8	872.3	921.2	1286.3	1314.1
Bundaberg	Australia	0.91	15.7	23.8	21.5	232.9	397.4	460.0	717.8	1044.0	1030.3
Brisbane	Australia	0.65	44.6	72.3	63.6	570.1	870.8	948.4	1035.1	1351.8	1335.2
Spring Bay	Australia	0.57	46.2	83.1	98.6	704.6	1054.7	1143.0	1184.4	1464.5	1495.8
Townsville	Australia	1.18	10.6	14.0	13.2	112.1	176.1	221.0	470.9	748.1	734.8
Broome	Australia	2.27	11.1	12.0	13.2	39.2	49.7	56.3	125.7	187.1	176.6
Cocos	Australia	0.51	180.9	238.1	330.0	1304.3	1519.5	1575.3	1596.9	1658.1	1701.9
Darwin	Australia	1.53	18.5	20.0	21.9	88.7	121.7	142.1	322.4	492.4	478.1
Esperance	Australia	0.74	23.0	29.9	39.1	453.8	647.9	787.6	1012.8	1276.6	1312.8
Fremantle	Australia	0.74	22.5	30.4	39.3	469.0	696.8	842.2	1094.9	1335.6	1397.0
Cananeia	Brazil	0.96	19.3	28.6	26.8	418.1	681.5	755.7	1124.4	1311.9	1381.4
Ilha Fiscal, RJ	Brazil	0.83	15.1	22.9	21.0	335.6	585.5	652.1	921.1	1162.0	1208.7
Victoria, BC	Canada	0.91	4.7	5.9	7.0	101.1	131.5	183.4	370.7	576.4	542.8
Prince Rupert	Canada	1.56	4.8	5.2	5.4	38.7	43.8	50.7	154.7	165.1	208.8
Tofino	Canada	1.11	1.7	2.1	2.4	30.5	37.9	50.5	128.7	197.3	180.0
St. John's-A	Canada	0.82	23.6	38.1	42.3	278.8	639.0	639.7	660.0	1075.5	1042.2
Halifax	Canada	0.84	34.5	48.1	57.2	437.5	842.7	911.5	965.0	1275.9	1392.6
Churchill	Canada	1.28	0.1	0.2	0.1	1.3	4.4	3.3	10.9	11.0	10.4
Puerto Montt	Chile	1.60	7.0	8.1	9.3	32.7	44.0	52.2	120.4	199.1	192.4
Juan Fernandez-B	Chile	0.52	32.3	44.5	53.1	579.7	759.3	911.6	1024.5	1239.3	1267.6
Antofagasta	Chile	0.48	20.1	38.1	43.1	453.7	684.4	807.5	862.0	1126.6	1157.5
Easter-C	Chile	0.59	11.2	18.4	18.8	510.5	699.6	822.7	1031.0	1249.9	1270.3
Valparaiso	Chile	0.53	13.4	22.2	24.4	262.2	452.5	551.9	658.9	939.8	964.9
Xiamen	China	1.43	6.3	7.3	8.7	71.2	91.9	129.0	313.5	489.1	502.5
Buenaventura	Colombia	1.06	22.2	27.1	27.5	194.8	293.9	342.2	638.9	910.9	894.4
Tumaco	Colombia	0.88	10.7	15.5	15.8	121.8	195.1	233.8	402.2	649.7	623.8
Cartagena	Colombia	0.25	1816.1	1747.8	1799.9	1825.7	1818.2	1826.0	1822.6	1808.5	1823.4
Penrhyn	Cook Islands	0.34	437.7	609.7	621.2	1549.6	1630.4	1672.8	1632.5	1688.9	1718.3
Quepos-A	Costa Rica	0.75	32.4	43.6	46.1	481.4	686.4	793.5	1019.8	1263.8	1274.2
Hornbaek	Denmark	1.25	4.3	42.8	3.8	37.5	287.1	45.7	171.1	347.4	190.8
Gedser	Denmark	1.29	3.8	23.4	3.4	40.4	228.1	51.0	201.0	315.9	237.0
Baltra-B	Ecuador	0.71	18.9	29.3	31.3	473.7	662.4	778.3	983.0	1224.1	1241.1
Santa Cruz	Ecuador	0.63	35.0	54.5	57.5	656.1	856.2	985.3	1119.2	1333.8	1353.8
La Libertad	Ecuador	0.74	51.1	73.6	75.6	954.1	1140.8	1276.9	1485.6	1587.5	1628.2
Acajutla-A	El Salvador	0.63	55.8	78.7	86.4	827.4	1037.5	1157.1	1305.1	1465.5	1489.2
Chuuk	Fd. St. Micronesia	0.40	202.5	274.0	298.8	1182.5	1390.0	1504.0	1417.4	1557.8	1596.3
Kapingamarangi	Fd. St. Micronesia	0.50	122.1	155.9	191.6	1176.0	1317.1	1451.6	1449.1	1582.2	1602.5
Pohnpei-B	Fd. St. Micronesia	0.51	127.3	166.3	175.5	1105.4	1310.7	1426.8	1418.6	1556.3	1587.8
Yap-B	Fd. St. Micronesia	0.54	70.9	96.5	109.9	951.8	1270.6	1369.6	1370.6	1527.1	1557.8
Suva-C	Fiji	0.51	269.0	317.3	333.3	1557.0	1513.7	1703.6	1731.1	1748.0	1720.1

Continued on next page

Table S-4 – continued from previous page

			10-yr Flood								
			2050			2100			2150		
Site	Region	Historical Height (m above MHHW)	AF 1.5°C	AF 2.0°C	AF 2.5°C	AF 1.5°C	AF 2.0°C	AF 2.5°C	AF 1.5°C	AF 2.0°C	AF 2.5°C
Noumea	France	0.43	208.1	307.2	291.3	1242.8	1415.9	1550.6	1452.0	1611.9	1572.7
Brest	France	1.70	8.6	7.9	9.3	37.5	50.9	54.4	137.5	207.4	165.2
Marseille	France	0.68	10.2	125.7	15.1	262.5	570.1	411.9	812.3	754.0	1046.2
Rikitea	French Polynesia	0.31	532.3	751.2	761.0	1571.6	1664.8	1686.9	1625.9	1705.8	1673.2
Papeete-B	French Polynesia	0.31	637.9	885.9	878.7	1672.5	1704.1	1762.1	1709.3	1752.2	1733.2
Cuxhaven	Germany	2.65	2.1	2.1	2.0	5.7	12.4	6.3	36.4	34.7	34.0
Malin Head	Ireland	1.27	4.6	5.0	3.8	32.5	56.9	34.8	135.6	128.7	138.0
Hakodate	Japan	0.48	34.8	56.6	111.6	509.7	717.1	872.1	874.6	1123.6	1141.5
Hamada	Japan	0.63	27.3	42.3	80.3	668.0	896.5	1030.5	1114.0	1359.0	1331.2
Maisaka	Japan	0.77	1.8	2.2	3.8	74.2	109.8	179.4	284.6	478.8	522.3
Ishigaki	Japan	0.78	22.7	31.9	54.8	627.5	784.4	958.3	1126.2	1336.7	1359.5
Naha	Japan	0.71	40.0	57.7	105.2	748.2	912.5	1111.4	1192.0	1382.8	1416.4
Toyama	Japan	0.47	172.8	260.0	421.9	1308.0	1476.0	1520.1	1521.7	1649.8	1609.0
Hosojima	Japan	0.81	6.1	8.2	13.8	196.5	305.1	415.5	575.4	846.4	872.8
Kushiro	Japan	0.52	1570.4	1537.4	1584.6	1826.1	1823.6	1826.1	1826.1	1822.4	1826.0
Abashiri	Japan	0.64	38.7	80.8	93.6	664.3	905.2	1014.8	1164.8	1334.2	1363.9
Mera	Japan	0.60	155.1	207.1	311.1	1511.8	1613.3	1615.1	1724.9	1747.7	1710.9
Wakkanai	Japan	0.53	125.1	215.6	312.1	1265.2	1491.4	1488.6	1563.2	1678.3	1639.2
Chichijima	Japan	0.57	107.0	229.6	321.6	1199.0	1303.5	1488.0	1522.3	1600.6	1621.0
Nishinoomote	Japan	0.71	38.5	51.8	92.1	710.7	902.5	1044.5	1182.9	1408.9	1397.1
Naze	Japan	0.73	63.0	79.5	139.1	947.6	1092.5	1288.0	1361.0	1520.9	1540.4
Hachinohe	Japan	0.50	396.3	509.4	671.4	1651.2	1743.0	1729.8	1779.9	1783.0	1770.1
Miyakejima	Japan	0.87	157.1	173.4	242.2	1658.2	1711.9	1701.7	1813.4	1806.8	1798.8
Nakano Shima	Japan	0.74	51.0	65.7	114.1	858.9	1017.1	1156.1	1297.8	1484.3	1464.0
Ofunato	Japan	0.50	1221.5	1376.5	1306.1	1824.9	1823.2	1819.2	1825.7	1823.4	1822.1
Nagasaki	Japan	0.83	29.8	37.0	49.8	403.9	565.3	687.5	873.0	1144.7	1140.9
Aburatsu	Japan	0.82	10.3	13.9	25.9	350.3	509.0	646.2	859.3	1137.3	1148.4
Kushimoto	Japan	0.68	85.6	112.7	182.0	1254.5	1435.6	1473.5	1610.4	1686.8	1667.5
Cendering	Malaysia	0.90	13.7	16.9	19.4	232.5	351.1	445.7	654.3	889.4	886.5
Johor Baharu	Malaysia	0.81	34.1	40.8	46.9	432.4	589.6	717.2	898.4	1130.0	1133.7
Kuantan	Malaysia	0.96	18.4	21.8	24.6	253.0	370.3	468.0	706.0	940.5	938.7
Keling	Malaysia	0.65	40.1	49.9	58.5	518.0	679.3	817.1	917.1	1136.6	1139.2
Lumut	Malaysia	0.76	25.8	33.4	40.7	407.7	563.3	672.2	832.6	1068.3	1060.1
Kelang	Malaysia	1.22	12.5	13.9	15.7	114.1	156.9	204.5	425.4	599.5	588.5
Langkawi	Malaysia	0.83	29.0	35.9	42.9	322.8	461.0	562.0	736.7	973.8	964.1
Penang	Malaysia	0.72	46.8	59.6	72.8	535.6	713.5	827.1	954.6	1183.7	1178.7
Port Louis-C	Mauritius	0.41	109.6	177.3	271.5	1038.2	1329.3	1377.1	1320.4	1522.8	1542.5
Rodrigues	Mauritius	0.69	27.8	41.7	56.5	699.4	919.4	1050.9	1229.9	1454.6	1461.8
Manzanillo-A	Mexico	0.52	261.1	377.0	405.5	1670.8	1692.5	1737.9	1777.3	1760.1	1776.8
Ensenada	Mexico	0.65	53.6	78.9	84.2	694.5	921.0	1028.5	1226.9	1387.9	1419.1
Salina Cruz	Mexico	0.53	126.7	183.0	195.9	1313.4	1456.9	1552.7	1581.8	1655.7	1677.6
Acapulco-A, Gro.	Mexico	0.51	437.5	596.6	645.7	1800.8	1782.9	1807.9	1819.0	1799.7	1811.1
Cabo San Lucas	Mexico	0.59	49.2	73.9	76.7	724.4	947.7	1051.6	1195.4	1376.2	1395.0
Guaymas	Mexico	0.52	180.4	255.8	346.6	1577.0	1639.3	1663.3	1746.1	1742.9	1761.3

Continued on next page

Table S-4 – continued from previous page

			10-yr Flood								
			2050			2100			2150		
Site	Region	Historical Height (m above MHHW)	AF 1.5°C	AF 2.0°C	AF 2.5°C	AF 1.5°C	AF 2.0°C	AF 2.5°C	AF 1.5°C	AF 2.0°C	AF 2.5°C
Saipan-B	N. Mariana Islands	0.44	125.2	186.6	209.5	1187.6	1311.4	1479.6	1398.0	1511.3	1584.4
Marsden Point	New Zealand	0.75	8.2	28.3	21.9	335.2	649.1	714.4	866.0	1254.1	1240.3
Tauranga	New Zealand	0.51	62.0	199.0	155.5	949.0	1307.1	1401.9	1272.3	1588.4	1596.8
Taranaki	New Zealand	1.10	3.8	7.8	6.5	88.7	194.1	214.7	439.4	757.9	733.1
Wellington	New Zealand	0.49	140.0	371.0	292.0	1311.5	1564.6	1626.5	1519.4	1720.1	1731.8
Tregde	Norway	0.77	11.5	17.5	9.8	112.7	215.3	143.5	350.2	407.7	450.3
Rorvik	Norway	1.15	1.5	3.2	1.7	17.2	36.0	22.3	77.5	86.1	76.7
Ny-Alesund	Norway	0.66	0.6	18.3	0.0	6.4	21.7	5.5	51.8	23.3	32.2
Vardo	Norway	1.03	3.7	15.1	5.7	37.5	111.6	64.6	135.6	234.3	184.0
Balboa	Panama	1.24	17.1	18.9	20.2	106.9	169.1	189.2	413.3	668.1	654.1
Cristobal	Panama	0.29	915.3	937.3	1108.2	1642.4	1711.5	1787.3	1635.2	1718.8	1750.3
Rabaul	Papua New Guinea	0.36	293.7	371.7	446.8	1360.1	1467.7	1597.7	1511.0	1628.0	1649.2
Lobos de Afuera	Peru	0.60	22.3	41.6	42.5	614.8	815.8	937.3	1060.7	1282.5	1300.7
Callao-B	Peru	0.46	29.3	57.1	66.4	687.4	885.0	1029.1	1054.0	1281.4	1307.1
Legaspi	Philippines	0.51	288.4	416.7	464.0	1616.7	1669.6	1742.3	1746.6	1740.0	1778.1
Manila	Philippines	0.69	424.1	546.3	613.1	1821.7	1815.2	1824.0	1825.5	1819.2	1825.5
Cascais	Portugal	0.93	17.1	15.4	21.6	156.3	236.4	313.1	556.8	790.4	802.6
Funchal-B	Portugal	0.64	93.9	84.8	129.6	739.2	930.6	1056.5	1170.9	1354.8	1459.1
Kanton-B	Rep. of Kiribati	0.43	122.4	191.0	199.9	1178.8	1349.5	1406.3	1409.2	1538.2	1577.7
Christmas-B	Rep. of Kiribati	0.42	209.0	322.3	333.7	1405.8	1490.2	1540.0	1541.7	1629.3	1659.5
Majuro-A	Rep. of Marshall I	0.60	110.2	139.8	137.8	1019.3	1207.0	1332.9	1396.9	1538.6	1577.0
Kwajalein	Rep. of Marshall I	0.51	222.8	274.2	283.6	1275.1	1460.0	1544.3	1533.4	1617.6	1669.9
Malakal-B	Republic of Belau	0.51	139.2	177.0	199.6	1069.9	1381.6	1450.4	1446.9	1590.3	1615.5
Kaohsiung	Republic of China	0.58	25.5	38.2	54.8	482.7	634.2	778.0	818.2	1049.7	1062.1
Keelung	Republic of China	0.67	24.0	36.9	68.0	774.9	945.7	1081.2	1174.9	1377.8	1376.7
Luderitz	South Africa	0.55	87.6	108.3	131.5	996.0	1228.5	1371.7	1350.3	1521.8	1581.8
Saldahna Bay	South Africa	0.60	79.4	93.1	113.5	825.8	1066.8	1184.7	1233.7	1438.8	1484.8
Simon's Town	South Africa	0.62	75.5	90.1	111.3	934.4	1185.8	1309.2	1371.6	1542.0	1593.1
Port Nolloth	South Africa	0.64	57.8	69.8	75.9	750.8	1000.9	1142.8	1222.7	1441.6	1499.4
Port Elizabeth	South Africa	0.76	24.8	34.2	36.2	418.9	623.9	752.6	919.5	1211.9	1241.4
La Coruna	Spain	1.07	23.4	21.1	25.3	157.3	222.3	263.8	559.7	751.3	757.2
Ceuta	Spain	0.45	49.7	73.1	104.3	633.5	791.4	1005.8	1050.0	1264.2	1344.7
Vigo	Spain	1.10	17.6	16.2	20.4	144.5	209.2	254.6	543.4	750.8	748.4
Stockholm	Sweden	0.76	2.9	233.3	1.5	31.6	465.6	34.0	85.0	13.6	101.1
Goteborg-Torsh.	Sweden	1.12	2.9	14.6	2.5	28.8	162.2	33.2	124.8	188.2	129.7
Zanzibar	Tanzania	1.06	30.4	35.2	37.4	201.8	288.5	365.2	577.0	839.3	851.7
Ko Lak	Thailand	0.93	30.1	36.0	40.0	413.9	576.0	690.9	950.9	1178.7	1181.8
Stornoway	United Kingdom	1.39	7.0	6.5	6.1	35.7	49.6	38.3	141.8	123.8	139.4
Lerwick	United Kingdom	0.84	9.8	12.3	8.1	90.6	136.9	100.6	289.2	288.7	326.8
Faraday	United Kingdom	0.80	4.7	7.0	5.2	41.0	49.1	83.2	280.7	537.2	563.1
Gibraltar-A	United Kingdom	0.43	49.2	69.5	99.3	508.8	671.9	872.4	899.4	1135.4	1213.4
Bermuda-B	United Kingdom	0.53	72.5	91.2	121.9	927.8	1072.9	1152.6	1304.8	1454.9	1430.6
Newlyn, Cornwall	United Kingdom	1.24	15.8	15.9	15.4	87.2	129.1	111.0	304.6	375.9	408.1
Seward-C, AK	USA	1.28	0.5	0.8	0.6	9.7	12.6	11.2	51.0	58.3	59.5

Continued on next page

Table S-4 – continued from previous page

			10-yr Flood								
			2050			2100			2150		
Site	Region	Historical Height (m above MHHW)	AF 1.5°C	AF 2.0°C	AF 2.5°C	AF 1.5°C	AF 2.0°C	AF 2.5°C	AF 1.5°C	AF 2.0°C	AF 2.5°C
Ketchikan, AK	USA	1.53	2.5	2.6	2.8	22.6	25.7	29.6	93.7	97.8	123.3
Valdez, AK	USA	1.29	0.2	0.4	0.3	6.2	8.6	6.9	35.1	42.6	40.5
Yakutat, AK	USA	1.26	0.0	0.0	0.0	2.7	3.6	3.0	16.4	16.1	16.6
Seldovia, AK	USA	1.79	0.1	0.1	0.1	0.7	0.8	0.7	10.7	11.3	10.9
Sitka, AK	USA	1.21	1.0	1.0	1.2	17.3	19.9	22.4	76.7	76.6	98.1
Sand Point, AK	USA	1.12	5.1	5.4	6.1	80.5	93.1	128.6	337.4	372.4	501.4
Dutch Harbor-B, AK	USA	0.72	0.8	1.0	1.3	39.5	48.7	64.9	133.0	148.3	204.6
Cordova-B, AK	USA	1.35	7.7	10.1	9.4	89.7	115.9	118.9	418.7	437.7	526.8
Kodiak Isl., AK	USA	1.09	0.1	0.1	0.2	3.9	4.4	4.3	20.1	19.9	20.9
Adak, AK	USA	0.78	4.7	6.0	6.6	91.0	119.3	160.8	278.8	310.4	421.3
San Francisco, CA	USA	0.68	20.8	33.5	37.4	527.3	731.2	864.1	1099.2	1296.5	1323.2
San Diego, CA	USA	0.68	56.7	80.5	86.6	681.7	910.2	1015.4	1245.3	1402.2	1436.1
Los Angeles, CA	USA	0.66	32.1	49.2	52.4	412.0	605.2	712.9	906.8	1136.6	1159.9
Crescent City, CA	USA	0.92	2.9	3.8	4.5	64.3	81.9	124.0	250.7	407.1	387.6
Monterey, CA	USA	0.68	21.8	34.2	39.4	442.6	634.4	756.6	972.2	1193.7	1214.1
Port San Luis, CA	USA	0.69	16.8	27.2	31.1	320.0	478.4	595.3	795.7	1039.5	1054.6
Santa Monica, CA	USA	0.70	28.4	43.7	46.8	427.0	619.9	728.6	955.8	1176.1	1199.6
La Jolla, CA	USA	0.66	56.2	82.2	88.7	713.8	945.6	1049.0	1264.4	1416.3	1449.4
New London, CT	USA	1.04	5.6	8.0	8.3	141.0	329.5	336.4	540.5	934.0	953.3
Fernandina Beach, FL	USA	0.92	13.1	15.0	18.6	238.7	458.4	506.3	799.6	1090.6	1157.7
St. Petersburg, FL	USA	0.79	9.4	22.1	14.9	435.4	738.5	840.6	1082.9	1320.2	1384.4
Pensacola, FL	USA	0.84	4.1	9.8	5.6	221.2	470.6	500.0	799.1	1105.9	1131.4
Mayport, FL	USA	0.61	71.8	78.1	109.1	807.4	1136.5	1256.4	1293.1	1463.7	1587.6
Limetree Bay, FL	USA	0.30	696.5	650.0	827.5	1634.2	1625.9	1730.4	1636.2	1674.1	1732.1
Key West, FL	USA	0.43	276.4	324.1	439.4	1470.3	1517.0	1689.0	1609.6	1652.7	1713.1
Fort Pulaski, GA	USA	0.76	53.5	56.3	77.1	666.0	1000.1	1109.0	1279.4	1462.2	1584.0
Hilo, HI	USA	0.42	503.3	596.0	721.0	1686.5	1719.0	1743.5	1734.5	1760.8	1750.6
French Frigate, HI	USA	0.38	362.6	527.7	579.9	1465.2	1610.7	1656.8	1550.5	1659.4	1656.6
Kahului, HI	USA	0.36	650.1	742.3	873.4	1678.4	1710.4	1740.8	1706.5	1745.7	1736.7
Mokuoloe, HI	USA	0.36	449.0	540.9	657.4	1566.5	1631.2	1675.3	1608.1	1697.0	1687.3
Honolulu-B, HI	USA	0.36	442.6	534.6	650.3	1564.9	1630.0	1674.5	1607.2	1696.3	1686.8
Nawiliwili, HI	USA	0.37	361.3	455.3	553.0	1486.1	1592.8	1628.3	1554.4	1665.9	1658.2
Grand Isle, LA	USA	1.02	19.2	38.8	31.0	1604.4	1640.5	1762.9	1823.4	1800.8	1823.3
Woods Hole, MA	USA	0.92	12.4	18.1	20.0	262.6	566.0	601.9	779.2	1118.9	1215.9
Nantucket, MA	USA	0.95	8.3	13.5	14.0	264.8	559.9	605.6	834.6	1154.7	1270.9
Boston, MA	USA	1.04	15.0	18.9	22.1	190.0	391.9	414.3	583.5	954.2	970.9
Portland, ME	USA	0.93	19.2	25.9	29.1	196.8	418.7	432.0	530.0	915.5	902.5
Eastport, ME	USA	1.27	18.8	23.3	26.5	112.2	236.1	230.3	323.3	667.9	535.3
Duck Pier, NC	USA	0.90	23.8	34.7	43.8	461.1	844.5	908.1	1157.7	1380.0	1518.5
Wilmington, NC	USA	0.58	47.3	95.6	104.2	798.3	1177.8	1268.7	1288.1	1468.2	1609.8
Atlantic City, NJ	USA	0.94	24.0	34.8	43.2	448.6	833.0	909.3	1135.4	1372.4	1540.7
Cape May, NJ	USA	0.88	25.9	33.8	43.4	465.9	882.1	954.3	1153.3	1379.6	1573.3
Montauk, NY	USA	0.94	12.4	18.2	20.5	271.2	563.8	619.7	833.5	1161.1	1285.0
New York, NY	USA	1.09	6.1	8.7	9.6	154.8	358.7	365.1	582.7	974.2	1010.1

Continued on next page

Table S-4 – continued from previous page

			10-yr Flood								
			2050			2100			2150		
Site	Region	Historical Height (m above MHHW)	AF 1.5°C	AF 2.0°C	AF 2.5°C	AF 1.5°C	AF 2.0°C	AF 2.5°C	AF 1.5°C	AF 2.0°C	AF 2.5°C
Charleston, OR	USA	0.96	6.7	8.2	9.7	124.2	160.1	238.2	462.9	675.5	658.9
South Beach, OR	USA	1.04	8.9	10.7	12.2	154.1	196.8	281.1	575.5	805.1	787.0
Astoria, OR	USA	1.00	3.3	4.2	4.8	58.8	73.7	106.6	230.1	377.0	346.3
Newport, RI	USA	0.85	23.5	32.4	38.4	360.7	700.7	780.7	907.9	1206.2	1340.0
Charleston, SC	USA	0.77	35.8	43.0	55.1	579.9	918.4	1023.3	1211.1	1430.0	1539.0
Galveston (Pier 21), TX	USA	0.98	14.2	29.9	20.8	928.2	1222.7	1371.5	1679.3	1686.9	1761.8
Rockport, TX	USA	0.63	141.8	236.8	247.7	1662.0	1699.0	1771.5	1797.2	1774.0	1813.2
Port Isabel, TX	USA	0.64	40.6	78.5	73.8	1059.9	1320.0	1465.2	1517.5	1612.8	1695.4
Galveston (P. Pier), TX	USA	1.14	8.2	15.5	10.9	546.7	872.5	984.8	1513.4	1590.8	1682.0
Chesapeake BBT, VA	USA	1.05	12.0	16.8	19.5	289.1	600.5	652.1	998.4	1269.7	1413.2
Neah Bay, WA	USA	1.11	1.3	1.7	2.0	24.7	30.9	41.8	105.5	160.2	142.6
Willapa Bay, WA	USA	1.38	2.6	3.0	3.3	33.5	40.8	56.0	162.0	254.0	232.4
Lewes, DE	USA	1.04	10.5	13.6	16.5	227.5	536.2	549.7	824.6	1158.6	1281.4
Apra Harbor, Guam	USA Trust	0.29	852.2	920.5	1119.1	1620.4	1653.0	1759.7	1685.9	1700.2	1748.4
Wake	USA Trust	0.52	107.9	206.3	179.3	1182.8	1349.6	1475.0	1432.9	1553.2	1594.8
Johnston	USA Trust	0.54	58.7	98.8	91.2	957.9	1177.3	1250.8	1272.2	1458.8	1483.4
Midway	USA Trust	0.61	24.2	58.8	67.2	758.4	966.6	1180.4	1185.1	1369.9	1407.6
Pago Pago	USA Trust	0.38	579.2	722.6	777.5	1715.7	1760.7	1768.3	1752.0	1774.3	1771.4
Charlotte Amalie, VI	USA Trust	0.31	618.5	584.8	740.8	1595.4	1590.4	1712.8	1619.7	1662.3	1726.1
San Juan, PR	USA Trust	0.33	575.6	545.9	701.2	1586.4	1585.0	1713.7	1628.6	1670.1	1731.8
Magueyes Island, PR	USA Trust	0.27	944.5	842.1	1046.0	1678.5	1642.5	1754.9	1659.1	1686.0	1740.4

Table S-5: Expected flood amplification factors (AF) for the 100-yr flood for 2050, 2100, and 2150 under 1.5°C, 2.0°C, and 2.5°C global mean surface temperature stabilization scenarios.

			100-yr Flood								
			2050			2100			2150		
Site	Region	Historical Height (m above MHHW)	AF 1.5°C	AF 2.0°C	AF 2.5°C	AF 1.5°C	AF 2.0°C	AF 2.5°C	AF 1.5°C	AF 2.0°C	AF 2.5°C
Buenos Aires	Argentina	3.07	1.6	1.7	1.7	3.8	5.2	5.6	95.7	149.6	128.9
Fort Denison	Australia	0.74	74.0	189.0	152.8	2542.8	4577.0	5531.0	7203.0	10865.5	11223.7
Bundaberg	Australia	1.24	6.1	10.8	9.1	508.6	887.6	1071.2	3179.6	5699.0	5496.6
Brisbane	Australia	0.78	101.7	201.5	167.3	3001.5	5219.8	5830.1	7968.1	11411.9	11242.4
Spring Bay	Australia	0.71	81.2	183.5	229.1	3382.9	6517.2	7076.8	9030.1	12442.5	12587.4
Townsville	Australia	1.36	25.5	39.1	35.1	539.1	845.8	1074.4	3008.8	5213.4	5065.9
Broome	Australia	2.41	40.1	47.1	53.5	266.1	351.1	401.4	972.6	1457.1	1368.6
Cocos	Australia	0.58	849.8	1126.4	1689.8	10928.1	13440.3	14313.3	14987.4	15998.4	16422.2
Darwin	Australia	1.69	43.1	55.8	64.5	531.6	740.8	868.4	2271.5	3566.9	3432.9
Esperance	Australia	0.81	121.8	158.1	211.5	3223.6	4821.1	6073.0	8802.3	11631.6	11861.0
Fremantle	Australia	0.89	46.3	67.2	93.1	2188.3	3628.9	4606.8	7868.5	10880.9	11144.6
Cananeia	Brazil	1.37	6.4	9.2	8.4	558.2	1228.1	1272.9	4708.5	7576.4	7335.4
Ilha Fiscal, RJ	Brazil	1.06	15.9	26.0	22.9	1025.3	2188.5	2342.6	5582.3	8439.0	8389.6
Victoria, BC	Canada	1.06	10.4	14.1	17.8	540.0	687.0	963.8	2486.3	4057.3	3735.3
Prince Rupert	Canada	1.74	10.6	11.9	12.6	210.8	242.4	276.1	1048.4	1107.4	1382.3
Tofino	Canada	1.29	2.6	3.6	4.6	174.9	206.8	268.7	884.3	1293.4	1162.9
St. John's-A	Canada	1.02	35.7	66.3	70.6	1166.0	3125.4	2932.8	3837.6	8127.2	6605.6
Halifax	Canada	1.16	19.9	31.4	34.0	1096.0	2993.2	2634.5	4401.8	8623.0	7766.9
Churchill	Canada	1.63	0.2	0.2	0.2	1.8	25.7	5.8	77.0	77.9	72.1
Puerto Montt	Chile	1.70	22.0	28.1	34.3	209.1	300.2	364.5	936.8	1584.8	1519.9
Juan Fernandez-B	Chile	0.61	89.6	140.9	172.3	3578.4	5278.6	6614.0	8541.8	11023.2	11217.8
Antofagasta	Chile	0.60	28.3	71.9	83.8	2205.9	3906.6	4764.0	6434.8	9279.2	9479.0
Easter-C	Chile	0.92	4.0	5.3	5.3	871.0	1390.8	1825.5	5196.1	7442.6	7908.2
Valparaiso	Chile	0.61	36.2	71.8	80.2	1595.7	3000.7	3743.6	5312.1	8140.9	8277.1
Xiamen	China	1.72	8.7	10.7	13.5	253.4	317.9	460.9	1588.4	2624.9	2734.7
Buenaventura	Colombia	1.20	57.2	88.4	88.9	1093.6	1698.8	1978.8	4615.7	7169.2	6882.2
Tumaco	Colombia	1.01	19.3	37.1	37.7	677.0	1112.8	1328.9	2873.0	4975.3	4675.1
Cartagena	Colombia	0.30	17415.6	16094.6	17176.9	18238.4	18116.9	18253.9	18198.6	18021.3	18218.0
Penrhyn	Cook Islands	0.53	244.9	464.1	384.5	9644.5	11494.0	12640.6	13623.0	15143.5	15438.9
Quepos-A	Costa Rica	0.79	229.7	311.7	328.5	4000.0	5913.7	6889.0	9489.3	12017.2	12115.8
Hornbaek	Denmark	1.50	8.1	200.0	7.0	166.9	1933.4	194.9	1007.3	2641.2	1003.8
Gedser	Denmark	1.72	4.0	58.4	3.7	109.2	914.6	127.9	812.9	1668.7	781.2
Baltra-B	Ecuador	0.80	76.9	122.9	127.6	3090.6	4669.4	5597.5	8256.7	10858.3	11005.8
Santa Cruz	Ecuador	0.70	165.1	269.0	286.5	4832.6	6747.0	7910.7	9931.9	12317.2	12491.0
La Libertad	Ecuador	0.85	185.8	282.8	285.1	6176.9	8310.8	9550.7	12931.6	14636.6	14967.8
Acajutla-A	El Salvador	0.71	249.0	364.7	405.3	5935.2	8116.5	9234.2	11575.8	13611.7	13798.1
Chuuk	Fd. St. Micronesia	0.63	93.9	153.5	136.5	5024.5	8055.6	9105.2	10345.1	12659.1	12949.8
Kapingamarangi	Fd. St. Micronesia	0.60	370.7	489.7	608.8	8602.9	10565.8	11892.7	12922.2	14635.5	14914.7
Pohnpei-B	Fd. St. Micronesia	0.63	327.7	451.9	453.8	7321.0	9974.5	11171.9	12247.0	14126.1	14473.3
Yap-B	Fd. St. Micronesia	1.20	1.9	2.0	2.1	588.8	1063.0	1437.7	3989.9	6360.5	6126.2
Suva-C	Fiji	0.63	676.9	845.7	873.2	12404.9	12672.6	14999.4	16038.2	16762.8	16397.8

Continued on next page

Table S-5 – continued from previous page

			100-yr Flood								
			2050			2100			2150		
Site	Region	Historical Height (m above MHHW)	AF 1.5°C	AF 2.0°C	AF 2.5°C	AF 1.5°C	AF 2.0°C	AF 2.5°C	AF 1.5°C	AF 2.0°C	AF 2.5°C
Noumea	France	0.50	893.1	1313.7	1252.1	10058.3	12285.0	13926.9	13310.3	15383.8	14906.0
Brest	France	1.82	35.8	31.3	40.7	248.8	347.0	373.5	1065.9	1632.2	1257.6
Marseille	France	0.87	15.6	506.2	21.7	955.6	4131.2	1427.3	4898.9	6665.8	6908.5
Rikitea	French Polynesia	0.32	4672.5	6819.2	6884.8	15472.8	16486.4	16732.2	16129.4	16989.8	16665.1
Papeete-B	French Polynesia	0.56	97.9	229.2	237.8	9207.3	11317.4	12597.7	13725.7	15603.6	15199.4
Cuxhaven	Germany	3.48	2.2	2.2	2.1	5.9	16.4	6.7	117.5	101.0	93.2
Malin Head	Ireland	1.51	6.4	7.7	4.7	149.2	267.7	146.4	845.7	755.3	783.9
Hakodate	Japan	0.56	121.4	206.8	481.2	3463.5	5053.1	6687.4	7381.0	9884.3	10167.9
Hamada	Japan	0.93	8.8	13.6	30.0	1588.7	2542.4	3719.3	6107.7	8879.3	9060.6
Maisaka	Japan	1.45	1.2	1.3	1.4	85.9	99.1	157.6	629.8	965.9	1061.2
Ishigaki	Japan	0.95	46.8	65.2	117.4	3098.8	4158.0	5698.0	8449.1	10967.0	11240.2
Naha	Japan	0.94	33.7	56.0	128.7	2828.9	4040.8	5781.7	8093.6	10611.9	10994.4
Toyama	Japan	0.61	286.0	502.4	1082.9	8545.6	10832.9	11987.9	12908.4	14962.6	14586.4
Hosojima	Japan	1.17	3.3	4.1	6.0	405.0	596.9	920.6	2361.4	4121.0	4431.1
Kushiro	Japan	0.67	5770.6	7626.4	8706.5	18242.0	18117.7	18238.4	18259.3	18172.3	18256.3
Abashiri	Japan	0.76	101.5	259.1	308.5	3936.8	5903.6	7085.2	9504.7	11563.3	11859.1
Mera	Japan	0.88	57.1	80.6	187.7	6567.0	8974.0	9846.8	13402.4	15161.9	14819.3
Wakkanai	Japan	0.75	76.6	177.2	347.2	6017.5	8104.0	9465.9	12020.7	14193.7	13929.1
Chichijima	Japan	0.85	35.2	139.0	220.5	5389.0	6648.4	8773.1	10891.1	12880.4	13115.3
Nishinoomote	Japan	0.89	57.3	84.3	179.3	3296.9	4810.2	6170.3	8703.6	11442.7	11587.2
Naze	Japan	1.00	40.0	55.9	125.3	3372.1	4686.5	6316.7	8986.2	11660.1	11951.1
Hachinohe	Japan	0.66	652.2	903.8	1707.6	12559.9	14667.9	14962.3	16400.9	17081.9	16887.6
Miyakejima	Japan	1.23	81.0	91.8	150.3	7494.5	9177.5	10099.1	15678.0	16699.8	16528.1
Nakano Shima	Japan	1.08	13.9	20.0	48.7	2240.7	3089.9	4294.0	7494.9	10168.7	10345.9
Ofunato	Japan	0.63	3985.9	5392.9	6782.0	18045.6	18091.0	17948.2	18250.3	18198.0	18151.4
Nagasaki	Japan	0.96	91.8	123.2	177.3	2309.8	3395.0	4464.3	6755.1	9504.3	9602.6
Aburatsu	Japan	1.18	5.5	6.9	10.9	658.9	977.1	1539.5	3773.4	6140.4	6470.8
Kushimoto	Japan	0.82	210.8	280.6	507.9	8081.8	10405.9	11402.8	14079.5	15630.5	15450.2
Cendering	Malaysia	1.10	20.5	27.1	32.8	973.1	1575.5	2104.6	4357.0	6496.5	6415.3
Johor Baharu	Malaysia	0.93	114.7	144.8	172.0	2646.4	3864.4	4925.7	7320.0	9686.8	9712.5
Kuantan	Malaysia	1.14	35.6	46.1	54.9	1182.9	1840.2	2439.9	4951.6	7159.9	7113.2
Keling	Malaysia	0.74	158.1	201.3	246.1	3616.4	4995.7	6253.9	7926.8	10129.8	10155.5
Lumut	Malaysia	0.84	123.2	163.9	202.9	2953.4	4220.8	5233.5	7256.8	9612.8	9513.9
Kelang	Malaysia	1.33	52.4	61.5	72.0	755.2	1038.1	1377.7	3384.3	4913.7	4799.3
Langkawi	Malaysia	0.91	144.8	189.4	231.5	2338.0	3451.5	4322.0	6369.0	8693.9	8597.9
Penang	Malaysia	0.84	151.3	205.6	263.4	3388.3	4805.1	5845.1	7879.7	10228.2	10157.7
Port Louis-C	Mauritius	0.46	548.2	945.1	1567.4	8746.7	11688.9	12436.9	12276.5	14568.0	14767.4
Rodrigues	Mauritius	1.01	9.4	15.7	22.3	1720.5	2622.5	3365.4	6871.2	9698.1	9788.4
Manzanillo-A	Mexico	0.63	686.2	1106.0	1163.5	14040.3	15038.2	15783.4	17026.6	17088.0	17308.2
Ensenada	Mexico	0.70	338.2	507.0	543.0	5593.0	7748.8	8880.4	11298.3	13157.1	13458.9
Salina Cruz	Mexico	0.69	190.2	295.0	320.5	7627.2	10012.8	11180.4	13303.4	14922.2	15125.8
Acapulco-A, Gro.	Mexico	0.71	290.9	514.5	537.1	14612.1	15421.8	16170.1	17587.1	17458.4	17647.2
Cabo San Lucas	Mexico	0.63	328.1	493.6	514.9	6135.7	8334.5	9398.6	11225.2	13194.9	13386.8
Guaymas	Mexico	0.63	485.0	755.7	1056.3	12349.1	13855.1	14445.8	16311.3	16737.0	16976.6

Continued on next page

Table S-5 – continued from previous page

			100-yr Flood								
			2050			2100			2150		
Site	Region	Historical Height (m above MHHW)	AF 1.5°C	AF 2.0°C	AF 2.5°C	AF 1.5°C	AF 2.0°C	AF 2.5°C	AF 1.5°C	AF 2.0°C	AF 2.5°C
Saipan-B	N. Mariana Islands	1.32	1.4	1.5	1.5	308.5	641.1	588.2	2289.5	4034.0	4145.6
Marsden Point	New Zealand	1.96	1.3	1.4	1.3	38.9	65.1	58.7	500.5	782.3	680.4
Tauranga	New Zealand	0.58	254.9	922.0	696.5	6984.8	10869.3	11863.1	11422.6	14968.9	14995.1
Taranaki	New Zealand	2.13	1.4	1.6	1.6	28.8	51.0	44.4	397.5	613.4	540.8
Wellington	New Zealand	0.59	397.5	1303.0	962.0	9211.1	12970.2	13810.8	13415.5	16356.1	16440.7
Tregde	Norway	0.99	12.7	35.2	10.6	449.5	925.4	537.7	2019.0	2231.5	2289.0
Rorvik	Norway	1.72	1.2	1.6	1.2	39.8	91.0	49.0	295.8	296.5	266.9
Ny-Alesund	Norway	0.76	1.9	136.8	0.1	52.5	179.2	45.0	463.2	207.5	287.2
Vardo	Norway	1.23	5.7	51.5	10.6	184.1	599.4	307.5	853.4	1471.2	1104.1
Balboa	Panama	1.33	85.2	101.9	109.9	762.7	1218.9	1353.8	3341.5	5591.5	5431.1
Cristobal	Panama	0.35	4108.3	5087.1	6243.1	14803.5	16196.8	17285.0	15516.3	16766.0	17118.4
Rabaul	Papua New Guinea	0.38	2202.9	2875.5	3499.5	12959.0	14228.3	15578.3	14822.4	16091.1	16294.8
Lobos de Afuera	Peru	0.68	87.1	171.6	176.3	4281.2	6157.2	7186.3	9177.0	11646.8	11793.0
Callao-B	Peru	0.62	26.8	71.3	87.6	3064.0	4690.2	5655.0	7598.6	10248.5	10467.0
Legaspi	Philippines	0.64	689.0	1114.7	1221.4	12315.1	14158.3	15446.9	16071.0	16618.9	17111.8
Manila	Philippines	0.84	1093.6	1505.3	1702.0	17367.2	17598.7	17960.9	18239.1	18087.3	18223.8
Cascais	Portugal	1.04	65.7	57.0	89.2	948.0	1472.5	1966.8	4178.2	6325.2	6243.5
Funchal-B	Portugal	0.68	665.3	600.7	934.1	6280.9	8180.3	9489.7	10988.8	12964.9	14017.0
Kanton-B	Rep. of Kiribati	0.55	243.1	403.9	427.1	7791.4	9903.5	10701.4	12014.4	13890.0	14278.4
Christmas-B	Rep. of Kiribati	0.48	911.0	1533.1	1574.7	12231.2	13488.8	14132.8	14586.3	15738.4	16052.9
Majuro-A	Rep. of Marshall I	0.63	838.2	1069.4	1047.0	9263.5	11246.1	12550.0	13498.3	15041.0	15443.4
Kwajalein	Rep. of Marshall I	0.54	1661.9	2085.6	2113.0	11845.5	13877.7	14831.2	14911.0	15887.9	16444.2
Malakal-B	Republic of Belau	0.54	999.5	1290.4	1444.0	9808.3	13034.9	13861.9	13992.7	15584.5	15820.2
Kaohsiung	Republic of China	0.80	14.5	24.3	42.1	1855.7	2710.9	3735.5	5372.6	7593.2	7765.6
Keelung	Republic of China	1.04	7.1	9.1	15.8	1721.3	2594.8	3510.5	6428.6	8832.0	9048.7
Luderitz	South Africa	0.61	458.6	574.9	704.3	7900.0	10339.8	11904.6	12388.8	14475.3	15083.9
Saldahna Bay	South Africa	0.62	655.6	773.2	943.9	7636.9	10054.6	11266.4	11958.9	14120.9	14576.4
Simon's Town	South Africa	0.72	269.4	339.8	425.1	6141.3	8623.2	10045.0	11775.4	14142.2	14630.1
Port Nolloth	South Africa	0.69	352.7	434.7	467.1	6018.1	8424.1	9825.3	11258.6	13736.3	14277.5
Port Elizabeth	South Africa	0.87	84.3	122.6	130.7	2446.5	3868.8	4964.6	7333.3	10394.5	10639.3
La Coruna	Spain	1.17	112.8	97.3	125.1	1050.5	1502.6	1798.9	4397.5	6120.9	6073.2
Ceuta	Spain	0.54	147.1	273.9	379.4	3718.6	5326.8	7051.5	8614.1	10996.1	11771.3
Vigo	Spain	1.37	16.1	14.4	20.7	474.8	727.1	882.7	2764.4	4124.0	3864.9
Stockholm	Sweden	0.98	3.1	1605.8	1.6	158.3	3866.6	162.5	536.3	100.1	605.1
Goteborg-Torsh.	Sweden	1.43	3.2	45.5	2.7	113.9	787.9	122.7	681.4	1076.7	619.5
Zanzibar	Tanzania	1.11	222.4	261.1	280.6	1660.9	2390.4	3059.0	5165.4	7698.0	7823.9
Ko Lak	Thailand	1.05	117.8	146.6	165.9	2564.9	3808.8	4761.4	7812.3	10177.9	10187.1
Stornoway	United Kingdom	1.50	28.8	26.5	23.6	245.7	346.0	256.4	1139.6	971.0	1080.2
Lerwick	United Kingdom	1.02	17.0	25.3	13.6	448.5	682.4	470.2	1870.7	1791.5	1930.3
Faraday	United Kingdom	1.19	1.9	2.2	2.0	13.9	18.0	37.4	579.7	2223.9	2099.3
Gibraltar-A	United Kingdom	0.53	119.4	230.0	322.5	2770.5	4187.1	5636.8	6996.6	9516.1	10133.9
Bermuda-B	United Kingdom	0.66	164.9	241.5	298.8	5611.6	7150.0	8131.5	10853.2	12681.1	12185.9
Newlyn, Cornwall	United Kingdom	1.34	73.3	73.5	70.9	599.2	906.4	759.5	2386.8	2930.9	3136.2
Seward-C, AK	USA	1.55	0.5	0.8	0.6	48.5	61.5	52.6	332.8	393.4	383.1

Continued on next page

Table S-5 – continued from previous page

			100-yr Flood								
			2050			2100			2150		
Site	Region	Historical Height (m above MHHW)	AF 1.5°C	AF 2.0°C	AF 2.5°C	AF 1.5°C	AF 2.0°C	AF 2.5°C	AF 1.5°C	AF 2.0°C	AF 2.5°C
Ketchikan, AK	USA	1.70	4.7	5.1	5.7	128.1	147.4	164.5	665.7	688.6	842.6
Valdez, AK	USA	1.51	0.3	0.6	0.3	37.2	49.2	39.7	258.6	315.7	287.5
Yakutat, AK	USA	1.37	0.0	0.0	0.0	14.9	28.3	16.7	146.3	141.1	144.4
Seldovia, AK	USA	2.10	0.1	0.1	0.1	2.2	2.8	2.3	79.1	85.2	78.6
Sitka, AK	USA	1.42	1.2	1.2	1.4	95.4	109.7	116.6	520.0	514.9	621.5
Sand Point, AK	USA	1.28	13.1	14.4	16.9	444.4	514.4	683.8	2302.5	2505.8	3504.8
Dutch Harbor-B, AK	USA	0.79	2.8	3.2	4.1	311.5	383.9	490.8	1150.2	1265.4	1710.8
Cordova-B, AK	USA	1.64	8.2	11.4	10.1	311.3	406.3	406.9	2121.7	2236.7	2706.9
Kodiak Isl., AK	USA	1.52	0.3	0.3	0.3	6.1	10.3	7.4	125.8	122.3	126.1
Adak, AK	USA	0.96	6.0	8.6	9.0	454.9	598.3	760.2	1785.3	1974.0	2752.1
San Francisco, CA	USA	0.89	20.7	39.6	42.1	1823.3	2758.9	3789.1	7063.3	9574.6	9629.9
San Diego, CA	USA	0.77	249.4	378.4	409.7	4589.5	6580.3	7673.4	10697.9	12691.8	13011.9
Los Angeles, CA	USA	0.72	168.0	285.6	303.7	3092.5	4691.0	5715.1	7958.2	10421.5	10575.5
Crescent City, CA	USA	1.10	4.7	6.9	8.4	329.2	400.4	604.8	1600.8	2592.4	2418.6
Monterey, CA	USA	0.81	49.0	92.6	105.3	2320.4	3533.9	4617.0	7377.1	9852.3	9937.1
Port San Luis, CA	USA	0.82	35.1	71.1	79.3	1693.0	2547.6	3502.1	5824.4	8377.4	8399.8
Santa Monica, CA	USA	0.84	54.9	112.8	116.2	2190.4	3355.7	4275.6	7059.2	9563.1	9654.0
La Jolla, CA	USA	0.72	327.4	492.6	533.5	5515.6	7712.7	8809.0	11490.9	13299.8	13633.6
New London, CT	USA	1.68	2.9	3.2	3.6	155.6	300.8	281.9	1031.5	2694.6	1706.5
Fernandina Beach, FL	USA	1.20	13.4	15.3	19.2	669.9	1379.4	1489.1	3993.0	6869.0	6668.8
St. Petersburg, FL	USA	1.54	2.1	2.3	2.3	190.1	365.1	339.0	1715.4	3620.5	3023.4
Pensacola, FL	USA	2.23	1.3	1.3	1.4	32.0	50.5	45.9	375.1	688.0	453.8
Mayport, FL	USA	0.79	93.2	121.0	172.2	3408.7	6302.9	7086.3	9440.2	12136.4	13088.3
Limetree Bay, FL	USA	0.88	2.0	2.7	2.4	1333.9	2503.3	2629.5	6559.3	9187.5	9575.8
Key West, FL	USA	0.67	91.1	175.2	197.6	6284.3	8905.2	10664.8	12006.7	14008.6	14614.5
Fort Pulaski, GA	USA	0.98	56.7	67.4	101.0	2352.9	4579.8	5141.2	8604.6	11498.5	12311.0
Hilo, HI	USA	0.55	1018.3	1286.5	1778.9	13772.9	14962.4	15590.6	15977.4	16863.3	16750.6
French Frigate, HI	USA	0.44	1585.8	2755.6	2907.1	13046.3	14904.3	15514.9	14740.9	16107.9	16072.8
Kahului, HI	USA	0.45	2203.3	2720.3	3559.6	14790.3	15690.8	16221.3	16039.3	16914.9	16808.8
Mokuoloe, HI	USA	0.41	2336.8	2972.8	3796.2	14345.2	15328.8	15919.7	15418.1	16573.7	16502.0
Honolulu-B, HI	USA	0.41	2288.7	2920.3	3732.4	14323.4	15312.1	15908.4	15407.6	16565.8	16496.3
Nawiliwili, HI	USA	0.53	408.5	567.5	740.0	9834.7	11852.7	12691.7	13099.8	14987.4	14967.3
Grand Isle, LA	USA	3.70	1.3	1.3	1.4	2.0	2.4	2.2	213.1	353.1	237.2
Woods Hole, MA	USA	1.31	8.1	10.6	11.6	525.7	1263.0	1148.7	2705.4	6116.4	5020.3
Nantucket, MA	USA	2.03	1.7	1.7	1.8	79.3	138.7	130.0	639.6	1478.5	902.8
Boston, MA	USA	1.41	9.3	12.0	13.7	452.7	952.4	952.8	2193.9	5046.5	3868.8
Portland, ME	USA	1.16	26.1	38.4	42.5	772.0	1748.1	1693.5	2849.2	6214.0	5109.9
Eastport, ME	USA	1.51	26.1	39.8	45.0	473.7	1082.2	1013.1	1806.9	4375.2	2922.4
Duck Pier, NC	USA	1.17	25.8	42.2	49.3	1311.4	3153.4	3397.8	6650.5	10067.6	10437.7
Wilmington, NC	USA	0.90	11.3	58.9	40.6	1509.8	3606.1	4054.4	6768.7	10082.3	10484.1
Atlantic City, NJ	USA	1.30	14.1	21.7	24.7	927.0	2332.7	2314.9	4953.8	8873.5	8760.8
Cape May, NJ	USA	1.17	24.4	33.5	41.2	1210.4	3345.0	3225.2	6092.6	9903.4	10465.0
Montauk, NY	USA	1.27	12.8	17.1	19.3	666.4	1504.0	1488.6	3391.5	7137.6	6538.6
New York, NY	USA	1.80	2.6	2.8	3.1	138.0	259.9	245.7	967.6	2498.4	1532.1

Continued on next page

Table S-5 – continued from previous page

			100-yr Flood								
			2050			2100			2150		
Site	Region	Historical Height (m above MHHW)	AF 1.5°C	AF 2.0°C	AF 2.5°C	AF 1.5°C	AF 2.0°C	AF 2.5°C	AF 1.5°C	AF 2.0°C	AF 2.5°C
Charleston, OR	USA	1.09	20.8	27.0	33.3	711.1	899.9	1379.6	3313.8	5117.7	4931.5
South Beach, OR	USA	1.23	18.5	23.8	28.1	696.8	869.4	1298.7	3578.9	5487.9	5244.4
Astoria, OR	USA	1.15	7.0	9.7	11.9	335.0	408.3	586.2	1583.4	2581.5	2326.1
Newport, RI	USA	1.18	13.8	21.9	22.7	860.9	2096.2	1980.9	3811.0	7640.1	7032.3
Charleston, SC	USA	1.16	8.0	11.5	13.3	865.5	1779.7	2087.7	5213.8	8353.3	8455.6
Galveston (Pier 21), TX	USA	1.85	3.0	3.2	3.2	216.1	448.7	417.7	3109.2	5934.6	5325.5
Rockport, TX	USA	1.18	5.7	13.6	7.1	1697.3	3931.9	4450.4	10313.5	13021.6	13464.6
Port Isabel, TX	USA	1.36	2.3	2.5	2.5	358.2	803.8	837.9	3580.4	6461.5	5865.2
Galveston (P. Pier), TX	USA	2.62	1.7	1.7	1.7	37.5	63.8	61.2	609.4	1213.0	856.4
Chesapeake BBT, VA	USA	1.53	6.5	7.8	9.1	386.1	881.5	922.6	3030.7	6147.3	5476.5
Neah Bay, WA	USA	1.24	2.4	3.8	5.2	168.4	201.4	265.5	807.5	1194.2	1053.1
Willapa Bay, WA	USA	1.74	2.7	3.2	3.6	113.1	127.9	177.7	747.7	1114.7	994.0
Lewes, DE	USA	1.59	4.2	4.8	5.5	256.8	652.8	605.9	1951.0	4669.4	3575.8
Apra Harbor, Guam	USA Trust	0.40	2125.7	2788.0	3372.7	13523.0	14744.7	16219.8	15396.9	16164.8	16764.4
Wake	USA Trust	1.00	4.2	29.7	6.8	1898.4	3156.2	3458.0	6520.4	9154.8	9473.0
Johnston	USA Trust	0.74	71.0	120.9	102.5	4510.1	6877.5	7501.6	9348.6	11785.2	12101.8
Midway	USA Trust	0.88	13.4	46.8	39.9	2185.3	3755.4	5136.5	7521.3	9986.8	10271.9
Pago Pago	USA Trust	0.45	2208.9	3382.2	3665.0	15823.0	16830.0	16978.0	16923.8	17456.9	17394.1
Charlotte Amalie, VI	USA Trust	0.64	56.0	76.3	85.1	4840.3	7220.3	8019.9	10661.5	12853.7	13519.8
San Juan, PR	USA Trust	0.57	171.0	214.1	257.2	7621.6	9766.5	11001.1	12471.7	14218.7	14985.5
Magueyes Island, PR	USA Trust	0.56	116.0	168.7	183.6	7002.7	9212.3	10381.2	11933.0	13864.4	14527.4

Table S-6: Expected flood amplification factors (AF) for the 500-yr flood for 2050, 2100, and 2150 under 1.5°C, 2.0°C, and 2.5°C global mean surface temperature stabilization scenarios.

			500-yr Flood								
			2050			2100			2150		
Site	Region	Historical Height (m above MHHW)	AF 1.5°C	AF 2.0°C	AF 2.5°C	AF 1.5°C	AF 2.0°C	AF 2.5°C	AF 1.5°C	AF 2.0°C	AF 2.5°C
Buenos Aires	Argentina	4.05	1.4	1.4	1.4	2.1	2.5	2.7	114.6	180.3	138.1
Fort Denison	Australia	0.81	140.5	429.6	323.5	8649.3	16123.9	19873.8	30225.0	48052.3	49762.5
Bundaberg	Australia	1.61	2.7	3.6	3.3	665.9	1002.4	1159.0	6239.1	11760.0	11111.4
Brisbane	Australia	0.89	104.4	261.1	201.9	8448.1	15684.0	17844.6	30889.7	48056.7	46981.0
Spring Bay	Australia	0.84	60.0	176.3	244.3	7958.9	18449.5	19846.2	33203.7	50567.9	50639.5
Townsville	Australia	1.49	33.5	61.3	51.7	1626.8	2518.0	3219.9	10861.1	19537.4	18869.4
Broome	Australia	2.50	85.6	107.6	126.3	986.1	1363.2	1586.5	4122.9	6203.4	5810.1
Cocos	Australia	0.65	1958.0	2546.6	4139.6	43909.2	56561.1	62643.3	69259.0	76339.7	78271.0
Darwin	Australia	1.83	40.7	59.7	70.5	1609.9	2322.3	2771.1	8357.8	13279.4	12654.3
Esperance	Australia	0.85	413.0	543.7	734.4	13232.3	20200.7	25945.4	40484.4	54894.6	55731.2
Fremantle	Australia	1.00	60.3	96.4	141.3	6270.9	10620.5	13973.1	29603.4	45299.6	45251.7
Cananeia	Brazil	1.79	3.4	4.0	3.9	495.9	1019.3	1007.0	7657.8	16509.4	13643.6
Ilha Fiscal, RJ	Brazil	1.24	13.3	22.0	19.1	2160.3	4752.8	4854.5	17847.6	30823.6	29175.2
Victoria, BC	Canada	1.14	19.3	28.1	37.7	2009.5	2498.2	3477.7	10122.1	16606.5	14999.5
Prince Rupert	Canada	1.84	18.2	20.7	22.4	752.0	870.2	974.1	4239.0	4457.0	5507.5
Tofino	Canada	1.39	3.7	5.3	7.5	661.0	775.3	981.2	3594.3	5176.1	4638.8
St. John's-A	Canada	1.20	27.2	56.6	58.5	2832.2	7481.8	7033.6	11938.1	29799.7	19925.7
Halifax	Canada	1.45	9.5	14.0	14.9	1852.9	4730.2	3983.4	10299.0	26082.2	17564.1
Churchill	Canada	1.94	0.2	0.3	0.3	1.6	23.4	5.0	282.3	276.2	259.8
Puerto Montt	Chile	1.76	46.1	65.4	82.6	774.3	1159.8	1435.0	4023.0	6896.6	6573.1
Juan Fernandez-B	Chile	0.69	115.8	210.1	264.1	11187.0	17942.3	23604.7	35908.8	48786.8	49458.1
Antofagasta	Chile	0.71	20.7	61.1	72.1	5740.8	10700.9	13566.5	23918.9	37939.5	38056.6
Easter-C	Chile	1.29	2.3	2.5	2.6	970.3	1351.1	1694.8	9936.0	16619.2	18445.9
Valparaiso	Chile	0.66	69.6	160.1	180.7	5901.1	11314.7	14270.5	23035.9	36904.8	37161.8
Xiamen	China	1.93	8.4	10.7	14.2	601.3	740.5	1133.8	4995.8	8171.5	8496.3
Buenaventura	Colombia	1.30	81.9	150.2	148.8	3598.2	5729.0	6624.4	17997.7	29581.2	27909.2
Tumaco	Colombia	1.11	22.6	51.3	50.9	2194.3	3645.2	4291.0	11067.3	19954.9	18413.6
Cartagena	Colombia	0.34	77164.9	69958.0	78217.0	90984.6	90137.6	91235.8	90812.4	89782.8	91017.1
Penrhyn	Cook Islands	0.75	50.8	177.5	75.4	18978.2	26800.6	32871.6	48939.6	60896.9	62077.4
Quepos-A	Costa Rica	0.81	960.8	1310.0	1381.3	18173.4	27379.4	31975.9	45697.4	58523.8	58995.0
Hornbaek	Denmark	1.65	12.4	653.9	10.2	541.1	7453.4	611.9	3749.3	11200.9	3511.6
Gedser	Denmark	2.02	4.1	116.0	3.7	256.4	2555.1	282.6	2308.0	5303.9	2100.0
Baltra-B	Ecuador	0.87	180.7	300.0	311.6	11000.5	17367.9	21171.3	35614.1	49127.9	49572.8
Santa Cruz	Ecuador	0.73	593.1	1007.8	1059.3	21138.3	30282.1	35746.0	47025.4	59364.5	60190.0
La Libertad	Ecuador	0.92	452.8	719.0	725.7	22430.5	32398.4	37712.2	58035.9	68550.3	69871.1
Acajutla-A	El Salvador	0.77	622.5	989.9	1089.5	22499.7	32654.1	37598.3	52280.4	63639.0	64561.5
Chuuk	Fd. St. Micronesia	1.01	3.0	4.8	3.2	4159.7	9376.6	10166.9	24077.9	35763.0	35998.8
Kapingamarangi	Fd. St. Micronesia	0.67	765.7	1032.3	1298.7	32780.5	43647.5	49632.2	58552.4	68626.0	69991.1
Pohnpei-B	Fd. St. Micronesia	0.72	556.1	786.6	761.2	25024.7	38395.8	43866.7	53733.5	64683.1	66171.7
Yap-B	Fd. St. Micronesia	2.64	1.2	1.3	1.2	29.7	137.2	148.4	1287.5	1900.4	1612.4
Suva-C	Fiji	0.73	1006.2	1301.6	1352.0	46453.7	50845.0	62450.7	73297.6	79385.0	77276.1

Continued on next page

Table S-6 – continued from previous page

			500-yr Flood								
			2050			2100			2150		
Site	Region	Historical Height (m above MHHW)	AF 1.5°C	AF 2.0°C	AF 2.5°C	AF 1.5°C	AF 2.0°C	AF 2.5°C	AF 1.5°C	AF 2.0°C	AF 2.5°C
Noumea	France	0.54	2716.1	3967.5	3795.2	43692.9	55365.7	64369.5	62814.9	74443.8	71836.0
Brest	France	1.87	115.4	97.7	134.9	1041.6	1469.7	1587.8	4800.2	7394.6	5620.2
Marseille	France	0.98	22.8	1545.3	32.2	2845.9	16949.3	4078.8	17836.1	31071.6	25817.0
Rikitea	French Polynesia	0.34	17769.8	27627.1	27724.8	74777.4	80591.4	82129.7	79346.0	84219.9	82615.2
Papeete-B	French Polynesia	0.94	2.9	3.9	3.8	7289.1	12427.6	14575.5	36066.2	50044.1	48578.7
Cuxhaven	Germany	4.09	2.0	2.1	2.0	5.7	14.1	6.5	294.0	248.7	222.8
Malin Head	Ireland	1.68	7.0	10.0	4.7	463.4	861.2	429.7	3062.6	2695.1	2733.3
Hakodate	Japan	0.61	306.9	552.7	1445.1	13464.2	19964.6	27948.1	32966.9	45433.9	47047.5
Hamada	Japan	1.30	2.8	3.3	4.5	1618.3	2299.6	3735.2	12026.5	20931.3	22583.2
Maisaka	Japan	2.48	1.1	1.1	1.2	1.9	3.6	14.3	749.8	944.4	912.8
Ishigaki	Japan	1.09	57.3	83.1	154.0	8209.6	11067.3	16926.9	31923.0	44837.0	46038.4
Naha	Japan	1.17	13.7	22.7	56.1	4885.3	7073.3	12090.8	24776.0	37374.6	38516.4
Toyama	Japan	0.75	196.6	415.9	1216.8	23548.6	33811.3	41563.2	51716.9	64782.3	63765.6
Hosojima	Japan	1.56	2.0	2.3	2.7	589.9	748.6	1109.7	4699.7	7966.2	8917.5
Kushiro	Japan	0.78	8512.9	14900.2	19000.6	90460.1	88966.1	90583.9	91285.0	90484.2	91212.0
Abashiri	Japan	0.85	162.1	513.4	610.4	12710.8	20272.1	25672.6	39882.6	50971.5	52256.1
Mera	Japan	1.20	9.5	11.6	22.8	7026.7	11955.7	16064.0	38523.0	52089.8	53518.6
Wakkanai	Japan	0.99	15.1	43.1	106.8	9517.2	13334.5	20652.1	39038.1	51548.3	52521.4
Chichijima	Japan	1.19	5.4	19.4	22.3	7002.6	9048.4	14424.1	29332.4	41111.9	42764.4
Nishinoomote	Japan	1.04	46.7	73.9	181.8	8063.7	12476.5	17797.7	31876.0	45726.1	47144.8
Naze	Japan	1.29	10.1	13.6	30.6	4535.2	6523.4	10243.3	24213.2	37680.9	38863.4
Hachinohe	Japan	0.82	455.1	641.7	1679.5	38015.3	49823.7	55645.8	70360.0	78037.2	77295.2
Miyakejima	Japan	1.68	8.7	9.5	14.5	5691.5	7779.2	11104.7	42015.4	55128.9	57206.1
Nakano Shima	Japan	1.55	2.8	3.1	4.3	1595.5	2033.6	3230.7	12922.6	21883.8	23538.5
Ofunato	Japan	0.74	5692.6	8106.9	14596.3	85635.4	88070.9	86722.2	91097.5	90633.4	90151.2
Nagasaki	Japan	1.05	155.0	230.5	380.2	7696.2	11484.2	15893.4	27698.3	40991.7	41803.5
Aburatsu	Japan	1.53	3.1	3.7	4.9	941.1	1229.0	1932.8	7726.6	13828.8	15228.5
Kushimoto	Japan	0.92	365.5	502.3	973.7	26794.1	37762.8	44224.2	61662.8	72109.4	71444.6
Cendering	Malaysia	1.29	12.8	17.3	22.4	2219.1	3586.5	4902.8	14357.5	22999.0	22493.2
Johor Baharu	Malaysia	1.00	266.2	353.6	435.4	9829.7	14816.3	19296.0	32162.4	43810.1	43972.5
Kuantan	Malaysia	1.29	33.8	45.8	58.8	3175.4	5016.7	6817.2	18037.4	27665.7	27214.0
Keling	Malaysia	0.80	390.5	514.9	642.1	13908.9	19823.4	25568.4	35632.2	46594.1	46660.6
Lumut	Malaysia	0.88	409.8	558.8	700.9	12477.2	18077.1	22858.0	33750.8	45350.8	44870.4
Kelang	Malaysia	1.40	130.7	162.4	196.4	2893.0	3988.5	5357.5	14546.5	21481.1	20934.8
Langkawi	Malaysia	0.97	385.7	542.3	685.2	9124.7	13723.9	17524.9	28361.7	39755.8	39224.2
Penang	Malaysia	0.94	225.7	349.7	480.9	11125.0	16447.1	20902.1	32935.2	44464.6	44063.9
Port Louis-C	Mauritius	0.49	1848.3	3257.4	5610.2	38976.8	53603.6	57972.4	58577.8	70815.7	71760.1
Rodrigues	Mauritius	1.42	2.8	3.2	3.9	1623.6	2260.9	2897.7	12859.2	21911.1	21991.9
Manzanillo-A	Mexico	0.72	1131.0	1937.6	2033.4	55303.8	64018.1	68917.4	79934.6	82282.4	83662.1
Ensenada	Mexico	0.73	1267.7	1954.2	2094.0	24514.4	34709.0	40349.5	53663.9	63585.7	65056.7
Salina Cruz	Mexico	0.89	50.1	106.9	101.5	14457.5	23775.3	27655.5	48136.9	60529.7	61396.3
Acapulco-A, Gro.	Mexico	0.90	118.8	271.7	237.9	39725.2	50443.3	56119.2	77573.4	80842.2	82411.1
Cabo San Lucas	Mexico	0.64	1468.5	2228.6	2324.3	29384.7	40279.6	45597.8	55212.5	65245.7	66217.7
Guaymas	Mexico	0.72	807.9	1353.9	1916.9	45643.1	55248.7	60049.0	75171.2	79552.5	80992.7

Continued on next page

Table S-6 – continued from previous page

			500-yr Flood								
			2050			2100			2150		
Site	Region	Historical Height (m above MHHW)	AF 1.5°C	AF 2.0°C	AF 2.5°C	AF 1.5°C	AF 2.0°C	AF 2.5°C	AF 1.5°C	AF 2.0°C	AF 2.5°C
Saipan-B	N. Mariana Islands	3.85	1.1	1.1	1.1	1.2	1.3	1.3	282.0	385.1	316.3
Marsden Point	New Zealand	5.38	1.1	1.1	1.1	1.2	1.2	1.2	1.3	21.3	1.4
Tauranga	New Zealand	0.63	667.2	2631.1	1973.5	27072.0	46343.4	51139.3	52363.9	71123.0	71050.7
Taranaki	New Zealand	3.99	1.2	1.2	1.2	1.4	1.5	1.6	183.3	200.9	173.9
Wellington	New Zealand	0.65	857.0	3345.0	2400.7	34912.3	54956.9	59242.1	61140.5	78363.7	78370.3
Tregde	Norway	1.18	9.3	28.4	7.7	1168.3	2385.1	1331.5	6488.8	6766.6	6707.0
Rorvik	Norway	2.39	1.1	1.2	1.1	11.5	131.0	14.3	643.0	591.0	520.2
Ny-Alesund	Norway	0.82	4.9	573.3	0.1	229.0	802.7	192.6	2165.0	961.3	1338.6
Vardo	Norway	1.37	6.6	93.7	13.9	594.2	1953.8	972.7	3144.4	5343.2	3985.6
Balboa	Panama	1.38	263.7	335.7	362.2	3156.8	5072.9	5620.0	14822.8	25219.9	24356.5
Cristobal	Panama	0.40	9278.2	13596.8	16804.0	65421.6	75619.8	82205.6	73819.6	81834.0	83668.5
Rabaul	Papua New Guinea	0.38	11014.3	14377.8	17497.4	64795.2	71141.3	77891.7	74111.8	80455.4	81473.9
Lobos de Afuera	Peru	0.72	276.2	573.8	575.1	17694.5	26444.9	31047.5	42506.6	55264.3	55909.7
Callao-B	Peru	0.80	8.2	21.4	24.4	5680.1	9493.2	11853.5	24474.1	37730.3	37804.3
Legaspi	Philippines	0.77	672.4	1280.7	1393.6	39288.3	52445.8	60979.7	70550.7	77203.3	79735.2
Manila	Philippines	0.98	1466.0	2092.1	2382.9	71211.7	78505.8	83330.9	90527.9	89315.4	90575.8
Cascais	Portugal	1.11	157.1	133.1	230.1	3470.9	5448.2	7299.2	17329.6	27031.0	26251.7
Funchal-B	Portugal	0.71	2580.3	2331.7	3677.8	27776.2	36911.4	43573.5	52316.2	62627.8	67887.2
Kanton-B	Rep. of Kiribati	0.66	300.1	460.6	522.5	23931.7	34077.5	38042.5	50457.3	61644.6	63473.8
Christmas-B	Rep. of Kiribati	0.52	2621.6	4558.7	4627.9	54577.5	61850.0	65740.1	69963.3	76608.6	78094.6
Majuro-A	Rep. of Marshall I	0.65	3486.6	4463.4	4341.8	43283.8	53465.3	60070.9	65882.6	73996.2	76056.2
Kwajalein	Rep. of Marshall I	0.55	7535.2	9514.0	9580.9	57710.2	68122.4	73093.5	73831.2	78943.6	81762.3
Malakal-B	Republic of Belau	0.56	4020.4	5228.4	5829.8	46135.4	62482.2	67019.1	68355.4	76810.0	77964.2
Kaohsiung	Republic of China	1.07	3.5	4.8	7.6	2745.8	4086.2	6102.2	14794.9	23462.8	23993.9
Keelung	Republic of China	1.43	3.4	3.8	4.9	1656.4	2444.9	3500.2	13853.1	22131.6	23450.5
Luderitz	South Africa	0.64	1614.5	2063.5	2531.6	34663.2	46826.7	54805.1	58991.6	70359.4	73323.0
Saldahna Bay	South Africa	0.63	2972.8	3519.5	4297.4	36671.4	48734.4	54863.8	58856.5	69929.0	72186.4
Simon's Town	South Africa	0.80	495.8	681.2	872.5	20788.9	31289.8	38108.3	51010.2	64791.4	66982.6
Port Nolloth	South Africa	0.72	1312.4	1631.3	1750.4	26278.7	37710.8	44505.3	53500.3	66525.6	69169.3
Port Elizabeth	South Africa	0.94	188.3	296.3	315.1	8572.9	13846.3	18411.2	31228.4	46492.7	47493.2
La Coruna	Spain	1.22	364.1	306.5	413.6	4292.4	6156.7	7399.9	19453.0	27394.6	26973.1
Ceuta	Spain	0.60	339.5	731.1	1008.9	12885.0	19906.2	26779.3	37106.1	49493.7	52859.9
Vigo	Spain	1.63	8.1	7.5	9.8	884.8	1383.2	1635.4	7279.0	11009.7	9524.1
Stockholm	Sweden	1.14	3.1	6292.0	1.6	526.3	16766.7	528.8	1993.9	418.2	2212.6
Goteborg-Torsh.	Sweden	1.69	2.7	51.3	2.2	296.8	2278.5	301.7	2120.0	3355.7	1873.8
Zanzibar	Tanzania	1.13	960.4	1144.4	1236.9	7677.9	11082.1	14232.0	24700.0	37153.7	37779.2
Ko Lak	Thailand	1.13	276.0	360.1	418.6	9199.4	14085.2	18055.8	33798.1	45554.8	45542.2
Stornoway	United Kingdom	1.56	81.1	74.4	62.4	1003.9	1428.9	1030.0	5066.7	4250.9	4684.9
Lerwick	United Kingdom	1.17	17.6	30.9	13.2	1336.2	2017.8	1346.9	6700.9	6205.4	6569.6
Faraday	United Kingdom	1.77	1.3	1.4	1.3	1.8	2.0	2.6	279.2	1830.0	1590.9
Gibraltar-A	United Kingdom	0.63	116.6	408.4	543.8	7593.1	12690.0	16945.0	26366.4	38980.4	41214.7
Bermuda-B	United Kingdom	0.79	177.3	347.4	366.9	15488.1	21459.5	25739.3	43454.5	52731.1	49505.4
Newlyn, Cornwall	United Kingdom	1.39	231.9	233.1	223.2	2478.0	3797.5	3131.7	10573.4	12929.0	13739.5
Seward-C, AK	USA	1.78	0.6	0.8	0.7	133.1	186.8	135.2	1223.6	1455.2	1350.9

Continued on next page

Table S-6 – continued from previous page

			500-yr Flood								
			2050			2100			2150		
Site	Region	Historical Height (m above MHHW)	AF 1.5°C	AF 2.0°C	AF 2.5°C	AF 1.5°C	AF 2.0°C	AF 2.5°C	AF 1.5°C	AF 2.0°C	AF 2.5°C
Ketchikan, AK	USA	1.81	6.4	6.5	7.8	446.7	522.4	559.6	2715.9	2786.7	3318.2
Valdez, AK	USA	1.69	0.3	0.6	0.4	88.2	169.3	92.6	1024.5	1258.7	1116.4
Yakutat, AK	USA	1.42	0.0	0.0	0.0	57.4	109.3	64.6	694.6	660.5	677.3
Seldovia, AK	USA	2.37	0.2	0.2	0.2	3.9	5.1	4.0	306.7	343.9	300.5
Sitka, AK	USA	1.55	1.5	1.4	1.7	338.6	395.8	400.5	2107.0	2082.7	2409.4
Sand Point, AK	USA	1.37	24.6	27.6	33.7	1609.8	1866.0	2447.9	9292.2	9977.8	14117.1
Dutch Harbor-B, AK	USA	0.82	8.9	9.7	12.8	1408.5	1743.0	2193.2	5431.6	5939.9	7931.9
Cordova-B, AK	USA	1.92	4.7	6.5	5.6	623.3	796.4	768.0	5696.0	6027.9	7050.1
Kodiak Isl., AK	USA	2.09	0.5	0.5	0.5	1.0	1.8	1.2	356.5	343.7	322.7
Adak, AK	USA	1.11	5.2	8.4	8.2	1383.2	1815.2	2132.2	6278.6	6874.7	9347.5
San Francisco, CA	USA	1.06	15.5	29.9	31.8	4100.7	5853.1	8906.2	22800.8	35021.0	34393.6
San Diego, CA	USA	0.82	685.6	1184.8	1254.6	18121.6	26799.8	32060.9	48584.5	59534.8	60938.9
Los Angeles, CA	USA	0.76	500.0	966.2	996.9	12694.3	19522.0	24339.8	36256.4	48891.0	49459.8
Crescent City, CA	USA	1.20	7.3	11.5	14.4	1169.1	1400.0	2108.9	6403.9	10043.0	9338.2
Monterey, CA	USA	0.90	75.9	161.7	185.9	7473.5	11305.8	15807.4	29701.9	42331.8	42333.4
Port San Luis, CA	USA	0.91	51.8	122.0	136.0	5535.8	8139.4	11871.8	23099.6	35399.1	34987.0
Santa Monica, CA	USA	0.96	52.0	135.9	135.7	6182.5	9383.3	12858.6	26153.0	38887.2	38665.6
La Jolla, CA	USA	0.76	1083.4	1715.4	1865.3	22921.9	33054.4	38521.9	53473.5	63448.4	65032.2
New London, CT	USA	2.32	2.1	2.1	2.4	180.9	251.4	291.2	1676.3	3542.3	2172.2
Fernandina Beach, FL	USA	1.47	7.1	8.4	10.1	1227.4	2412.2	2486.5	9862.5	19474.0	16696.3
St. Petersburg, FL	USA	2.61	1.4	1.5	1.5	49.6	156.3	142.7	1325.6	2260.5	1578.4
Pensacola, FL	USA	4.97	1.1	1.1	1.1	1.2	1.3	1.3	121.9	167.6	110.6
Mayport, FL	USA	0.95	57.6	93.4	124.3	7375.9	15849.8	17493.3	33130.5	48435.1	50600.1
Limetree Bay, FL	USA	2.46	1.2	1.1	1.2	108.3	139.3	138.7	1367.8	2040.6	1641.1
Key West, FL	USA	0.96	7.9	31.9	16.6	6715.3	14048.9	15782.9	33432.6	48509.5	49892.8
Fort Pulaski, GA	USA	1.17	33.9	43.5	65.2	4763.4	9952.9	11180.8	27439.7	43026.5	43911.6
Hilo, HI	USA	0.67	1101.0	1398.0	2054.7	48909.9	58668.3	64368.1	71676.9	78764.7	78545.2
French Frigate, HI	USA	0.47	5112.1	9501.6	9810.6	60720.3	71033.6	74442.4	71625.4	79126.1	78932.7
Kahului, HI	USA	0.52	4370.1	5496.7	7507.0	63429.8	70423.9	74299.0	75574.3	81667.8	81311.8
Mokuoloe, HI	USA	0.44	7846.7	10190.2	13258.2	67323.2	73246.4	76634.2	75038.4	81544.9	81232.8
Honolulu-B, HI	USA	0.45	6664.0	8728.3	11408.8	65557.3	71928.3	75504.8	74255.5	81007.5	80723.4
Nawiliwili, HI	USA	0.71	224.1	262.8	392.7	23574.0	33271.0	38319.2	49882.4	62393.3	62933.5
Grand Isle, LA	USA	10.00	1.3	1.2	1.3	1.4	1.4	1.4	1.5	1.6	1.6
Woods Hole, MA	USA	1.65	5.2	6.5	7.2	890.1	1945.4	1658.5	5841.4	15392.8	9538.4
Nantucket, MA	USA	3.74	1.2	1.3	1.3	1.7	1.9	2.0	390.1	651.2	417.8
Boston, MA	USA	1.75	5.1	6.2	7.0	782.7	1499.7	1401.0	5036.4	12481.3	7633.6
Portland, ME	USA	1.33	26.3	41.8	44.3	2054.5	4493.9	4260.2	9109.6	22304.1	15760.2
Eastport, ME	USA	1.72	19.3	33.7	34.5	1154.2	2723.6	2423.1	5694.6	14587.3	8648.3
Duck Pier, NC	USA	1.40	17.9	29.9	35.3	2492.5	5948.8	6505.1	18241.9	34590.0	31860.1
Wilmington, NC	USA	1.24	3.9	7.7	6.0	1782.8	4022.9	4379.2	13403.3	27017.5	23543.8
Atlantic City, NJ	USA	1.62	8.0	10.9	12.6	1407.0	3299.1	3205.9	10439.6	24855.3	19048.4
Cape May, NJ	USA	1.43	14.5	19.6	24.3	2118.9	5730.6	5395.8	14979.9	32360.6	28499.7
Montauk, NY	USA	1.53	10.6	13.7	16.0	1350.4	2788.1	2665.4	8412.9	21327.4	15755.3
New York, NY	USA	2.61	1.8	1.9	2.0	93.3	172.3	183.6	1300.5	2547.7	1560.4

Continued on next page

Table S-6 – continued from previous page

			500-yr Flood								
			2050			2100			2150		
Site	Region	Historical Height (m above MHHW)	AF 1.5°C	AF 2.0°C	AF 2.5°C	AF 1.5°C	AF 2.0°C	AF 2.5°C	AF 1.5°C	AF 2.0°C	AF 2.5°C
Charleston, OR	USA	1.18	37.7	53.8	70.5	2505.9	3108.4	4800.4	13168.6	20908.5	19984.6
South Beach, OR	USA	1.37	22.2	31.1	38.2	2037.2	2469.1	3720.7	12483.4	19973.4	18772.7
Astoria, OR	USA	1.25	9.9	15.3	20.0	1179.6	1421.2	2048.2	6321.3	10045.6	9001.4
Newport, RI	USA	1.46	8.3	11.7	12.4	1572.1	3427.3	3138.9	8996.1	22403.0	16090.1
Charleston, SC	USA	1.61	3.0	3.2	3.6	835.1	1508.4	1703.2	7925.2	15785.5	13080.1
Galveston (Pier 21), TX	USA	2.96	1.9	1.9	1.9	33.4	155.6	138.6	1648.4	3005.7	1985.6
Rockport, TX	USA	1.97	2.1	2.2	2.3	510.5	923.3	913.8	7270.5	15475.8	11903.8
Port Isabel, TX	USA	2.76	1.3	1.3	1.3	7.5	126.3	115.7	1251.6	2014.6	1396.5
Galveston (P. Pier), TX	USA	5.26	1.3	1.2	1.3	1.6	1.7	1.7	152.5	211.6	145.1
Chesapeake BBT, VA	USA	2.02	3.4	3.7	4.2	461.4	909.9	895.4	4740.5	10662.9	7203.3
Neah Bay, WA	USA	1.31	4.2	7.1	10.8	686.8	818.8	1061.3	3497.6	5115.0	4501.7
Willapa Bay, WA	USA	2.05	2.2	2.6	2.8	251.3	269.6	382.2	2185.3	3014.1	2590.3
Lewes, DE	USA	2.18	2.5	2.6	2.9	269.9	551.6	557.6	2789.4	6303.5	4022.3
Apra Harbor, Guam	USA Trust	0.50	2417.4	3602.8	3793.9	51797.9	62775.5	70531.0	69295.5	75780.4	78992.1
Wake	USA Trust	1.82	1.5	1.6	1.7	618.0	927.2	813.2	5042.8	8596.8	8543.8
Johnston	USA Trust	0.89	45.7	171.4	76.8	11344.6	20089.5	22332.8	35174.6	47531.8	49323.9
Midway	USA Trust	1.12	7.5	16.1	14.8	3714.3	6376.9	9526.7	22321.2	34381.6	34488.4
Pago Pago	USA Trust	0.48	7167.3	11780.5	12692.2	75498.9	81710.1	82693.4	82939.5	86495.5	86097.5
Charlotte Amalie, VI	USA Trust	1.24	1.8	1.7	1.8	1590.1	2712.5	2494.8	13142.3	23022.3	22474.6
San Juan, PR	USA Trust	0.93	4.4	8.7	5.7	5947.9	11394.3	11413.4	31020.1	44208.2	46298.4
Magueyes Island, PR	USA Trust	1.09	1.9	1.9	2.0	2508.2	4807.1	4466.8	18458.3	30861.5	31125.9